

# PARTICLE WORLD

Technical Papers of QUANTACHROME

Edition 3 • May 2009

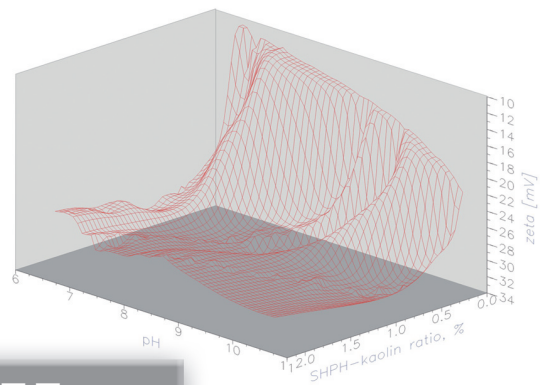
## Analysis instruments for characterization of concentrated dispersions

**Applications:** Nano particles, emulsions, cement and ceramic slurries, milling processes and stability of dispersions

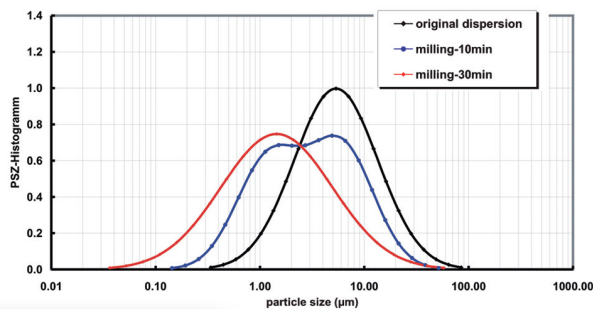
## Near-process characterization of dispersions

## Particle size and zeta potential of dispersions in original concentration

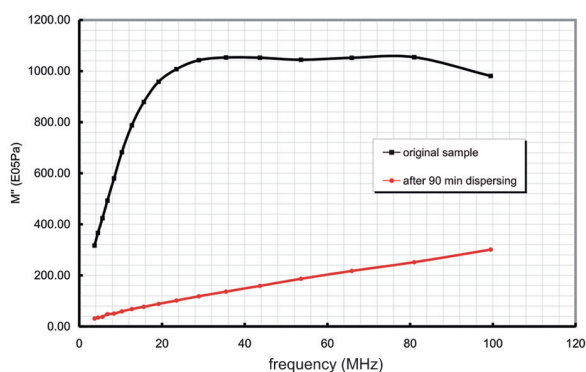
### ZETA POTENTIAL



### PARTICLE SIZE



### RHEOLOGY



Dear Reader,



forty years ago the classical methods for particle size analysis were replaced by laser diffraction devices manufactured by the French company CILAS. The application of optical waves to particle size analysis is described in the ISO 13320. In addition to optical techniques the acoustic waves can be applied very successfully to particle size characterization, especially in research on dispersions. The particular advantage of these acoustic techniques is the possibility to measure liquid, concentrated dispersions: **This allows a near-process characterization of the sample in its original state.** Ten years ago that very possibility led to the breakthrough invention of the acoustic spectrometers DT-1200 and DT-100 (particle size, ISO 20998-1) and the electroacoustic device DT-300.

The PARTICLE WORLD gives a comprehensive overview of the acoustic measurement methods for the calculation of particle size and zeta potential in concentrated liquid dispersions using DT-100, DT-300 and DT-1200. In addition to the instruments specifications you'll find an overview of their capabilities and optional enhancements. In the following paragraphs we present a selection of different applications of acoustic techniques on samples in their original concentration. These results clarify the outstanding capabilities of the applied acoustic methods in comparison with other techniques. The presented applications include stability tests on dispersions, online measurements on the grinding process, characterization of cement slurries as well as research on emulsions.

In order not to go beyond the scope of this journal, a more detailed presentation of combined examinations of dispersions and fine particles was abandoned. As the head of LabSPA (Laboratory for Scientific Particle Analysis) I'd like further to remark, that we offer an excellent combination of measurement methods thanks to our cooperation with the manufacturing companies [www.cilas.com](http://www.cilas.com), [www.dispersion.com](http://www.dispersion.com), [www.formulaction.com](http://www.formulaction.com) and [www.quantachrome.com](http://www.quantachrome.com). This situation enables us to provide a comprehensive characterization of dispersions, powders and porous structures.

All measurement techniques are offered as direct sample testing service for research or commercial purposes alike or they could be combined with for the method development service – please use the enclosed fax form to specify your request! In the second part of the PARTICLE WORLD you'll find the detailed description of the working method and theoretical background to the acoustic and electroacoustic spectrometry. Especially I'd like to draw your attention to a novelty, **for the first time we'll present the acoustic rheometer DT-600. This rheological option can be included in the combined device DT-1200.**

I trust that the PARTICLE WORLD will be an informative and interesting read for you!

With best wishes

Yours Christian Oetzel

**Articles in this issue:**

Overview of the acoustic analysis methods for the calculation of particle size, zeta potential and rheological parameters in concentrated dispersions . . . . . 3

Acoustic and electroacoustic spectrometers and their application

1. Research on stability of dispersions. . . . . 5

2. Particle size analysis of different nanoscaled powders . . 6

3. Investigation of the milling process in an on-line experiment . . . . . 7

4. Analysis of the state of dispersion . . . . . 8

5. Particle size analysis of powder mixtures . . . . . 9

6. Characterization of cement dispersions using ultrasound techniques . . . . . 10

7. Rheological analysis of dispersions . . . . . 12

8. Rigid materials in emulsions . . . . . 13

9. Colloidal properties of coarse, „non-colloidal“, highly-dense particles. . . . . 14

Near-process particle size measurement using the acoustic spectrometers DT-100 and DT-1200 . . . . . 15

Near-process measurement of colloidal properties (zeta potential) by means of the electroacoustic devices DT-300 and DT-1200 . . . . . 21

News:

Measuring the visco-elastic properties using the acoustic rheometers DT-600 and DT-1200 . . . . . 27

Imprint . . . . . 31

## Overview of the acoustic analysis methods

for the calculation of particle size, zeta potential and rheological parameters in concentrated dispersions

### DT-1200

Combined acoustic/electroacoustic instrument DT-1200 consisting of the DT-100, DT-300 and DT-600 (as an option)



- Provides all the possibilities of the individual devices to determine particle size, zeta potential and rheological parameters (as an option)
- Combi-measurement cell for particle size and zeta potential
- Can be equipped with additional probes for temperature, pH-, permittivity-, electric conductivity- and rheology-measurement as well as with the non-aqueous option and an automatic software controlled titrator
- Simultaneous operation of the probes
- Uniform data handling

### DT-100

Acoustic spectrometer DT-100 for particle size measurement



- Characterization of suspensions and emulsions; aqueous, polar and non-polar solvents
- Extended measurement range: 5 nm – 1000 µm
- Measurement of the non-diluted original sample (0,1 – 50 vol.-%)
- No calibration necessary
- Frequency range: 1 to 100 MHz
- Variable sender-detector-gap
- Data management via Access-database

### DT-300

Electroacoustic probe DT-300 for zeta potential measurement



- Characterization of suspensions and emulsions; aqueous, polar and non-polar solvents
- Measurement of the non-diluted original sample (0,1 – 50 vol.-%)
- Minimal sample volume: 2 ml
- Determination of the dynamic mobility and double layer thickness (Debye length)
- Data management via Access-database

### DT-600

Acoustic rheometer DT-600 to measure rheological properties



- Characterization of suspensions and emulsions; aqueous, polar and non-polar solvents
- Measurement of the longitudinal modulus  $G^*$  in the frequency area 1 – 100 MHz
- Measurement of the non-diluted original sample (0,1 – 50 vol.-%)
- Newtonian tests
- Determination of the volume viscosity
- Data management via Access-database

## Specifications

	<b>DT-100</b> Particle size	<b>DT-300</b> Zeta potential	<b>DT-600</b> Rheology	<b>DT-1200</b> Particle size and zeta potential
<b>Calculated parameter</b>				
Mean size (µm)	0,005-1000	-	-	0,005-1000
Lognormal parameter	Yes	-	-	Yes
Bimodal parameter	Yes	-	-	Yes
Zeta potential (mV)	-	± (0,5% + 0,1)	-	± (0,5% + 0,1)
Longitudinal viscosity (cP)	-	-	0,5-20000 ±3%	optional
Bulk viscosity–Newtonian systems (cP)	-	-	0,5-100 ±3%	optional
Liquid compressibility 104/Pa-1	-	-	1-30 ±3%	optional
Newtonian test – MHz range	-	-	any	optional
<b>Measured parameters</b>				
Temperature (°C)	0 -100, ±0,1°C	0 -100, ±0,1°C	0 -100, ±0,1°C	0 -100, ±0,1°C
pH	0,5-13,5, ±0,1	0,5-13,5, ±0,1	0,5-13,5, ±0,1	0,5-13,5, ±0,1
Frequency range (MHz)	1-100	1-100	1-100	1-100
Acoustic attenuation (dB/cm MHz)	0-20, ±0,01	-	0-20, ±0,01	0-20, ±0,01
Sound speed (m/s)	500-3000, ±0,1	-	500-3000, ±0,1	500-3000, ±0,1
Electroacoustic signal	-	±1%	-	±1%
Electric conductivity (S/m)	10 <sup>-4</sup> -10 <sup>1</sup> , ±1%	10 <sup>-4</sup> -10 <sup>1</sup> , ±1%	-	10 <sup>-4</sup> -10 <sup>1</sup> , ±1%
<b>Measurement time (min)</b>				
Particle size	1-10	-	1-10	1-10
Zeta potential – aqueous systems	-	0,5	-	0,5
Zeta potential – non-aqueous systems	-	0,5-5	-	0,5-5
<b>Sample requirements</b>				
Sample amount (ml)	20-70	2-100	20-100	20-110
Volume fraction %	0,1-50	0,1-50	no restrictions	0,1-50
Electric conductivity	no restrictions	no restrictions	no restrictions	no restrictions
pH	0,5-13,5	0,5-13,5	0,5-13,5	0,5-13,5
temperature (°C)	< 50	< 50	< 50	< 50
Viscosity medium (cP)	up to 20000	up to 20000	up to 20000	up to 20000
Micro-viscosity medium (cP)	up to 100	up to 100	not restricted	up to 100
Viscosity colloid (cP)	up to 20000	up to 20000	up to 20000	up to 20000
Particle size (µm)	0,005-1000	0,005-100	not restricted	0,005-1000
Zeta potential (mV)	no restrictions	no restrictions	no restrictions	no restrictions
<b>Physical specification</b>				
Output (power)	100-250 VAC 50-60 Hz, < 300W	100-250 VAC 50-60 Hz, < 300W	100-250 VAC 50-60 Hz, < 300W	100-250 VAC 50-60 Hz, < 300W
<b>Available options</b>				
pH-temperature option	Yes	Yes	Yes	Yes
Electric conductivity probe	Yes	Yes	Yes	Yes
Permittivity measurement system	Yes	Yes	Yes	Yes
Peristaltic pump	Yes	Yes	Yes	Yes
Automatic titration	Yes	Yes	Yes	Yes
Non-aqueous application	Yes	Yes	Yes	Yes

1 Measurement device can measure systems with a higher content than 50 vol.-%, but the theory for the determination of PSD and zeta potential is strictly applicable up to 50 vol.-%. In some systems with a low density contrast it is the lowest volume fraction 1 %.

2 The decisive viscosity for particle size- and zeta potential-measurements is the one, at which the particle expires, when it moves into the acoustic field. This „micro-viscosity“ can be – for gelatinous or structured systems e.g. – much smaller than the value measured by means of a conventional rheometer. In this case, the sphere of influence exceeds clearly the dimension of the particle.

3 Particle size measurement range for the zeta potential can depend on the density contrast.

## Acoustic and electroacoustic spectrometers and their applications

### 1. Research on stability of dispersions

Dispersions show different destabilization effects. Some of them are shown in figure 1.1. It is difficult to find an adequate definition for „stability of a dispersion“ because there are different processes, which can play a role. One possibility is the following:

The primary particle structure will be conserved in case of a stable dispersion – the preconditions will be a small density contrast  $\Delta\rho$  between the continuous and the dispersed phase. Furthermore, the particle size  $\varnothing$  should be smaller than 1  $\mu\text{m}$  and the zeta potential  $\zeta$  should be bigger than 30 mV. On the other hand the primary particle structure will not be conserved in case of an unstable dispersion and will be irreversibly modified. The term redispersible dispersion means, that the particles are flocculated in the so-called secondary minimum – a redispersion is possible in this case. The above definition leads to the conclusion, that one parameter in the statement „stable“ is not sufficient. It is rather the combination of different methods, which allows real analysis of stability.

Aqueous dispersions of titanium oxide (AV01, Anatas) with 20 wt.-% solids content were prepared for the following stability test. Thereby the influence of different dispersion methods on particle size and colloidal properties was investigated. The dispersion methods were

- Ultrasound deflocculation (Bandelin, Sonotrode HD 2200)
- Addition of an additive (BYK 180®)
- pH variation by means of HCl and KOH

In figure 1.2 the measured acoustic attenuation spectra of different treated dispersions are shown. Obviously a smooth spectrum with a characteristic frequency (maximum of attenuation) at about 30 MHz is obtained after a deflocculation by means of ultrasound. This shape is characteristic for a mean particle size in the submicron range (100 nm – 1  $\mu\text{m}$ ). The addition of the additive BYK 180 up to 2 wt.-%dwb (dwb = „dry weight basis“) doesn't cause a significant change of the spectrum, even if the viscosity of the dispersion decreases considerably. Only the spectrum of the sample with 10 wt.-%dwb BYK 180 shows a remarkable flattening of the curve – the dispersion changes to a polymodal particle distribution because of aggregation. An increase of the pH, exemplarily demonstrated between pH 7,6 and pH 10,8, leads to an additional flattening of the graph.

In figure 1.3 the influence of the ultrasound treatment on the particle size distribution is given. Figure 1.4 demonstrates the effect of the change in pH via KOH addition using the example of the 10 wt.-%dwb Byk-180 sample.

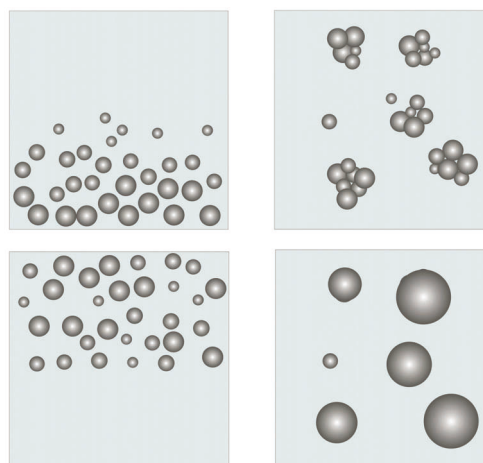


Figure 1.1 Different destabilization effects on dispersions: sedimentation and agglomeration (above) and creaming and coalescence (below)

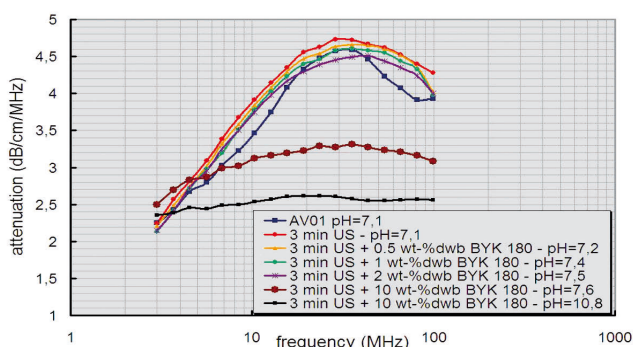


Figure 1.2 Acoustic attenuation spectra of 20 wt.-%, aqueous  $\text{TiO}_2$ -dispersions, treated in a different way

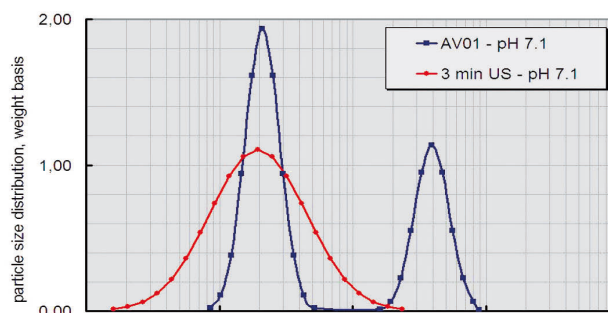


Figure 1.3 Effect of the ultrasound treatment on the particle size distribution of the 20 wt.-%, aqueous  $\text{TiO}_2$ -dispersion

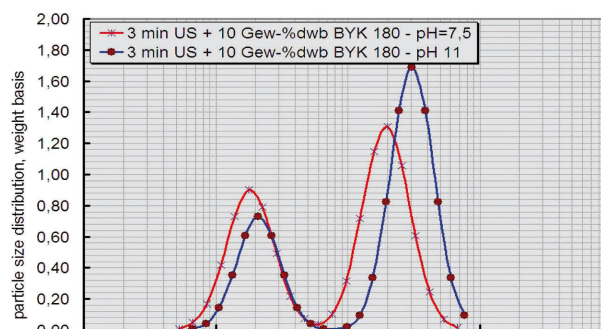
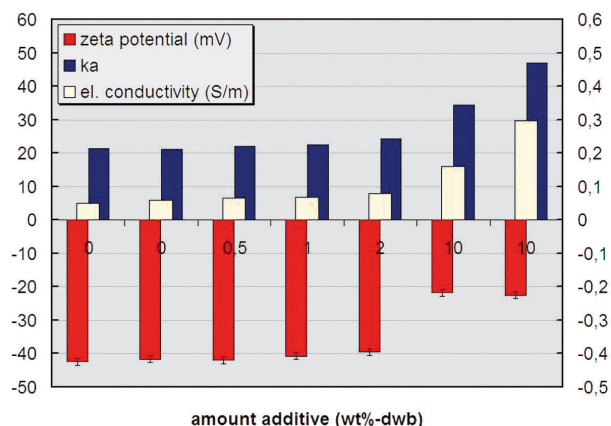


Figure 1.4 Influence of the ultrasound-treatment on the particle size distribution of the 20 wt.-% aqueous  $\text{TiO}_2$ -dispersion

The sonotrode destroys the existing micro scaled agglomerates and produces a monomodal distribution. The addition of 1 and 2 wt.-% BYK-180 doesn't change the particle size while the 10 wt.-% BYK-180 leads to a flocculation, which will be further increased by increasing the pH.

Some results of the coincidental to the particle size measured colloidal properties are given in figure 1.5. Here the zeta potential (mV) and the electric conductivity dependence on the added amount of the additive Byk-180 is shown. Furthermore the relation of the double layer thickness  $1/\kappa$  to the particle size  $a$  is given.



**Figure 1.5** Colloidal properties of the 20 wt.-%, aqueous  $TiO_2$ -dispersion, deflocculated in a different way: 1. ultrasound treatment; 2. Addition of Byk-180 (0, 0.5, 1, 2 and 10 wt.-%dwb); 3. pH increasing from 7,5 to 11

The zeta potential doesn't change significantly by adding an additive. On the other hand the viscosity decreased visibly between 0 to 2 wt.-% Byk 180 fraction: correspondingly the polymer acts as a steric stabilizer. At 10 wt.-%dwb fraction, the viscosity increases and the system is flocculating due to the high content of the polymer in the dispersion (depletion flocculation). The increase of the pH enhances this effect. The electric conductivity increases in each case, the zeta potential decreases. The  $\kappa a$ -parameter increases strongly, the double layer starts to shrink.

## 2. Particle size measurement of different nanoscaled powders

The characterization of nanoscaled particles aimed at obtaining the particle size distribution is challenging for any measuring method. For traditional fractionating techniques like sieving or filtering, these particles are much too small. For counting methods, very expensive high-resolution electronic microscopes are necessary. Additionally these visual analysis systems result in bad statistics. In case of optical systems, the tendency to agglomeration and/ or aggregation leads to problems, Optical waves „see“ these strong agglomerates or weak aggregates as coarse particles and a good dispersion is often very tricky. Furthermore if a near process characterization is necessary, the acoustic spectrometry is the most suitable method.

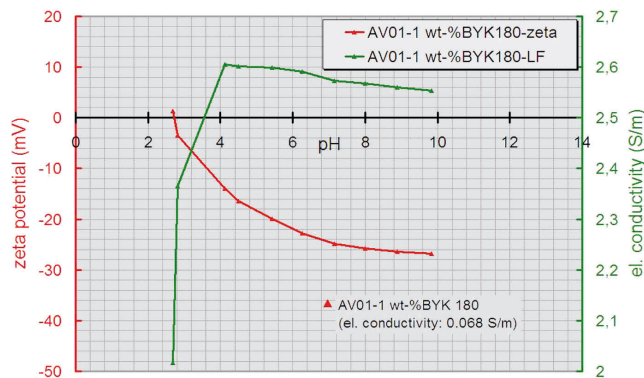


**Figure 1.6** Zeta potential and electric conductivity dependence on the pH (HCl and KOH) of the 20 wt.-%, aqueous  $TiO_2$ -dispersion with an amount of additive of 1 wt.-%dwb

Figure 1.6 demonstrates exemplarily the development of the zeta potential and the electric conductivity dependence on the pH (HCl and KOH) of a dispersion with an amount of additive of 1 wt.-%dwb.

From the initial state (pH = 7,3, Conductivity = 0,068 S/m, zeta potential = -39,24 mV) a pH of 2,7 was adjusted using HCl. Then the pH was gradually titrated to pH = 9,9 using KOH. Obviously the system shows a hysteretic effect: the curve stays below the zeta potential of the initial state over the complete pH range. The reason for this is the significant increase of the charge carrier concentration due to the addition of HCl and KOH respectively: the electric double layer is shrinking, the zeta potential decreases.

## Conclusion

To get an optimal stabilization and minimization of the viscosity of this suspension, it is recommended to disperse the powder in a weak basic medium using a small amount of the additive BYK 180. An exact adjustment of the additive-amount as well as of the pH can be realized by carrying out further series of measurement. By means of the DT-1200 the presented samples can be easily analysed in high concentrations.

Three aqueous dispersions with different, nanoscaled particles were prepared: a 5 wt.-% iron oxide-, a 5 wt.-% silver- and a 10 wt.-% silica-suspension respectively. 25 ml of the original dispersions were poured into the measurement cell of a DT-100. The samples were analyzed regarding their attenuation spectra without stirring. All measurements were repeated twice in order to test the stability of the sample in the limits of the measurement period. The measured spectra are given in figure 2.1. Beyond the intrinsic attenuation spectrum of pure water is shown. All dispersions are stable in the limits of the measurement period. The only attenuation effect, which plays a role here due to the small size of the particles, is the viscous effect (see below). This effect is sufficiently strong in case of the nano-silver and the nano-silica suspension. The shape of both curves is characteristic for nanoscaled particle

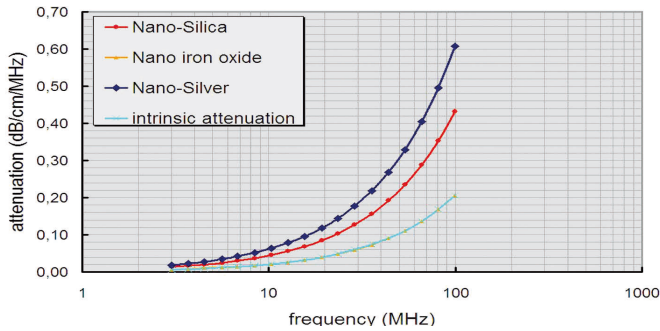


Figure 2.1 Attenuation spectra of the silica-, iron oxide and silver suspension in comparison with the intrinsic spectrum of water

systems. The spectrum of the iron oxide on the other hand is almost identical as the one for water: the particle size is too small for the measurement, at least smaller than 5 nm. Figure 2.2 shows the particle size distributions of three powders calculated from the attenuation spectra of figure 2.1. Table 2.1 summarizes the results in numbers.

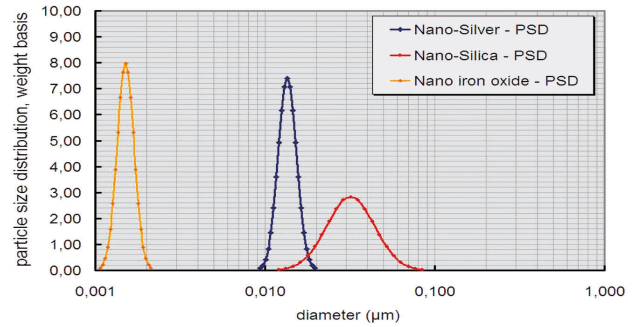


Figure 2.2 Particle size distributions of the silica-, iron oxide- and silver-suspension

### Conclusion

By means of the ultrasound spectrometer DT-1200, particle size distribution of concentrated dispersions with very small particles can be analysed. The shape of the attenuation spectra can give information about the size of the particles in the dispersion.

Results – particle size of nano-powders										
	Max-Mode 1 (µm)	Max-Mode 2 (µm)	Mean value (µm)	St.dev.	vfr2/vfr	d10 µm	d16 µm	d50 µm	d84 µm	d90 µm
Silica	0,032	-	0,032	0,14	-	0,022	0,024	0,032	0,044	0,048
Iron oxide	0,0015	-	0,0015	0,05	-	0,0013	0,0014	0,0015	0,0017	0,0018
Silver	0,014	-	0,014	0,05	-	0,011	0,012	0,014	0,015	0,016

Table 2.1 results of the particle size measurements of the silica-, iron- and silver-suspension

### 3. Investigation of the milling process in an on-line experiment

The DT-100 can be used for particle size distribution analysis via bypass experiment in order to control a milling process due to the possibility of a near-process measurement of concentrated dispersions. This is shown in figure 3.1. After the data acquisition and -analysis, the milling process parameters can be adjusted. In this article, a milling process of a CaCO<sub>3</sub>-dispersion will be discussed exemplarily. For this purpose a non-milled CaCO<sub>3</sub>-powder was milled using a commercial pearl mill. The particle size distribution was measured every 10 minutes by means of the DT-1200.

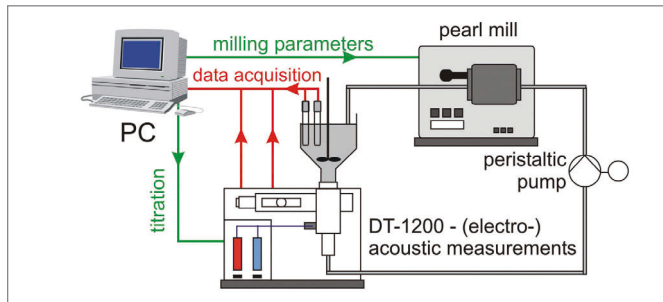


Figure 3.1 Schema of the bypass experiment of a milling process using a DT-1200

Figure 3.2 is showing the measurement data (acoustic attenuation) of the particle size measurement in dependence of the grinding time. Obviously the unground educts show a huge attenuation in the frequency range bigger than 20 MHz, which decrease significantly with an increasing grinding time. In the lower frequency range (smaller than 20 MHz), the effect is the inverse, the spectrum increases with an increasing grinding time. The explanation is given in figure 3.3. Two effects are responsible for the attenuation of the ultrasound: scattering at the CaCO<sub>3</sub>-particles and viscous friction at the particle-water boundary – both processes interfere with each other. The scattering is predominant for bigger particles (> 5 µm),

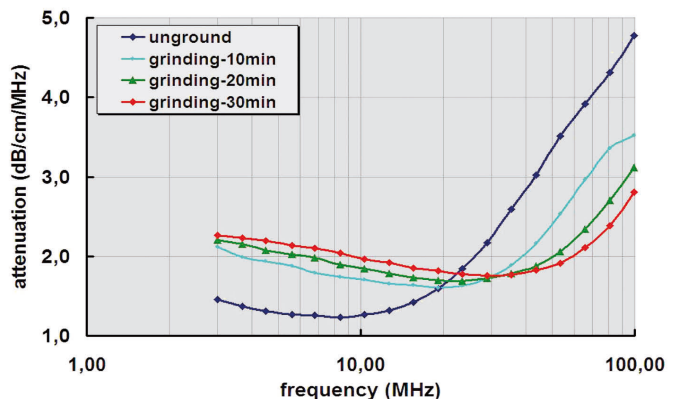


Figure 3.2 Influence of the grinding time on the acoustic attenuation spectra of the chalk sample

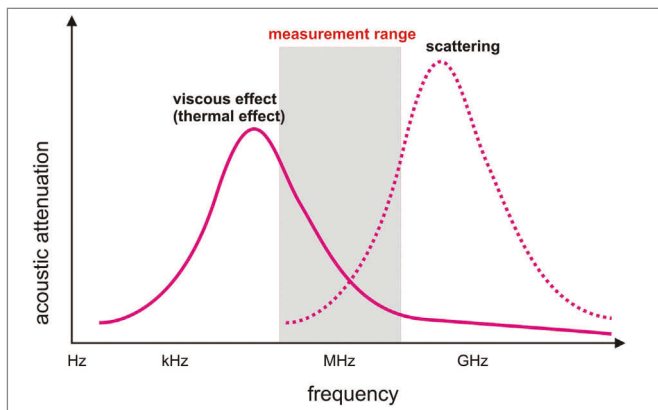
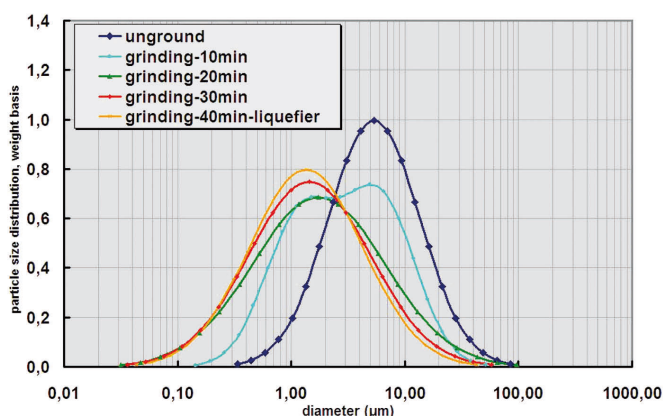


Figure 3.3 Interference of the attenuation mechanism viscous effect and scattering



while the viscous loss is the important effect for smaller particles. In the current example, the scattering forms the higher frequency range and the viscous loss the lower frequency part of the spectrum. Thus the attenuation spectrum decreases in the higher frequency range with an increasing grinding time, because the scattering effect of the particles decreases – for the viscous loss the situation is conversely.

Figure 3.4 shows the particle size distributions calculated from the spectra of figure 3.2. Starting with a size of about 6 µm and a lognormal distribution, a fine fraction is appearing after a grinding time of about 10 minutes with a maximum at 1,5 µm. After 20 minutes grinding, the coarser fraction is disappeared. A further milling of about 10 minutes doesn't lead to a further significant improvement.

### Conclusion

By means of the ultrasound spectrometer DT-1200 an online characterization of milling processes is possible. These processes can be controlled in high concentrations as well as in the range of nanoscaled particles.

Figure 3.4 Particle size distribution of the CaCO<sub>3</sub>-particles in dependence of the grinding period

## 4. Analysis of the state of dispersion

Agglomerates can be broken using dispersing techniques like ultrasound- or high-speed dissolvers as well as pearl mills. To avoid the reagglomeration, additives were applied, which can stabilize in an electrostatic, steric or electrosteric way.

In the following example, the state of dispersion of a 35-wt.%, aqueous titanium oxide dispersion (Hombitec, primary particle size about 30 nm) was examined. For this purpose, a basis suspension was prepared. 10 wt.-%dwb of BYK 190 was added to water, then 35 wt.-% of Hombitec was stirred into the liquid. Afterwards, the acoustic attenuation spectrum of this dispersion was measured (0-sample). Then the dispersion was, in a first step, deflocculated for 45 minutes using an agitator ball mill (Netzsch LabStar, Zeta geometry in ZrO<sub>2</sub>, diameter of the grinding element 0,65 mm YTZ), then again for further 45 minutes. The measured attenuation spectra for each measurement are given in figure 4.2. At first it is peculiar, that the complete spectrum between 1 and 100 MHz drops off. This is due to the crushing of bigger agglomerates to almost primary particles. From the particle size distribution one can observe, that these agglomerates are in the range of 200 to 300 nm – they are showing a maximum attenuation at 30 to 50 MHz. After the deflocculation they are disappeared. The resulting particles with a size of 30 to 40 nm are showing

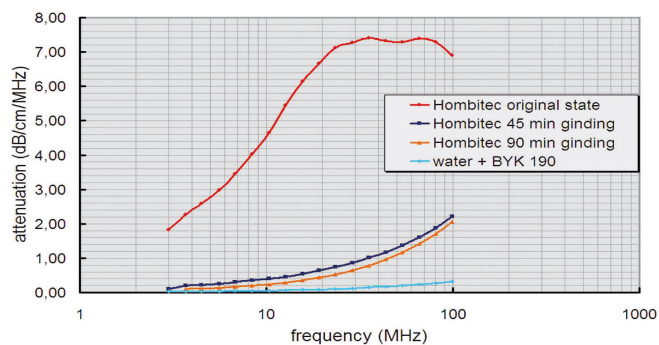


Figure 4.1 Attenuation spectra of 35 wt.-% aqueous dispersions of nanoscaled TiO<sub>2</sub> (Hombitec) – without, after 45 and after 90 min milling

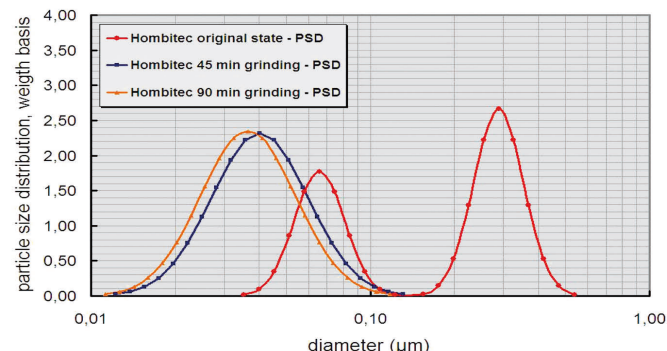


Figure 4.2 Particle size distribution of 35 wt.-% aqueous dispersions of nanoscaled TiO<sub>2</sub> (Hombitec) – without, after 45 and after 90 min milling



a much weaker attenuation. Further a maximum is not visible in the measurement range.

Sedimentation tests were carried out on all three dispersions using a TURBISCAN LAb Expert (see [www.formulaction.com](http://www.formulaction.com)). Figure 4.3 shows the level of the clarification zone (measured from the surface of the dispersion) in dependence of the holding time. Apparently sedimentation starts immediately in case of the 0-sample, while the 45 and 90 minutes milled samples are absolutely stable for at least 3 hours before they are starting to sediment. Furthermore there is no visual noticeable sedimentation for these two samples (figure 4.4). On the other hand figure 4.3 clarifies by means of the patented measurement principle of the TURBISCAN LAb Expert, that there are differences in the sedimentation behaviour of all three samples. A dispersion of 90 minutes shows an additional increase of the stability against sedimentation.

### Conclusion

The state of flocculation of dispersions can be analysed using a DT-1200 in the original concentrated dispersion. The TURBISCAN LAb provides additional information about destabilization processes like sedimentation, clarification or particle agglomeration by means of a time depending analysis of transmission- and backscattered signals of a laser light.

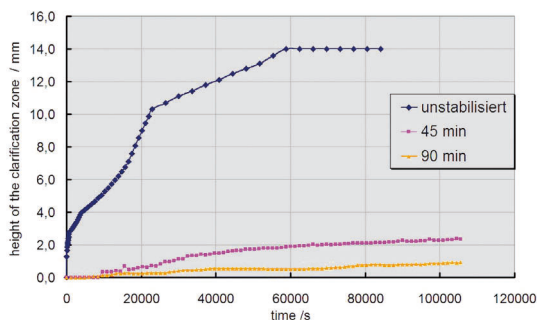


Figure 4.3 Stability tests (sedimentation) by means of the TURBISCAN LAb Expert on 35 wt.-% aqueous dispersions of nanoscaled TiO<sub>2</sub> (Hombitec) – without, after 45 and after 90 min milling



Figure 4.4 Photos of the three samples from the figure 4.3 after 30 hours sedimentation

## 5. Particle size analysis of powder mixtures

### 5.1 Mixtures of nanoscaled powders with the same basic raw material

A difficult job is the particle size analysis in the nanoscaled range in powder mixtures. In the following example, acoustic attenuation measurements were carried out at aqueous dispersions of two nanoscaled silica powders (Aerosile OX 50<sup>®</sup> and A 380<sup>®</sup>) and their mixtures. The primary particle size of OX 50 is about 50 nm and of A 380 about 10 nm. Figure 5.1 shows exemplarily the attenuation spectra of aqueous dispersions with 20 wt.-% solids content with OX 50, A 380 and mixtures with 25 and 50 wt.-% A380 fraction respectively. The four attenuation spectra differ clearly in their run. The attenuation at higher frequencies (> 30 MHz) decrease with an increasing fine powder content and flatten. All curves don't show a maximum in the frequency spectrum 1 to 100 MHz.

Figure 5.2 demonstrates the analysed particles size distributions of the 4 dispersions: the mean particle sizes are shifted to smaller values with an increasing fine powder content. At the same time, the standard deviation is increasing.

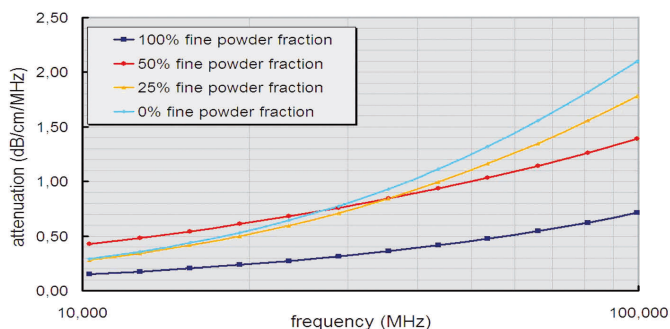


Figure 5.1 Acoustic attenuation spectra of 20 wt.-% aqueous dispersions containing different mixtures of OX 50 and A 380

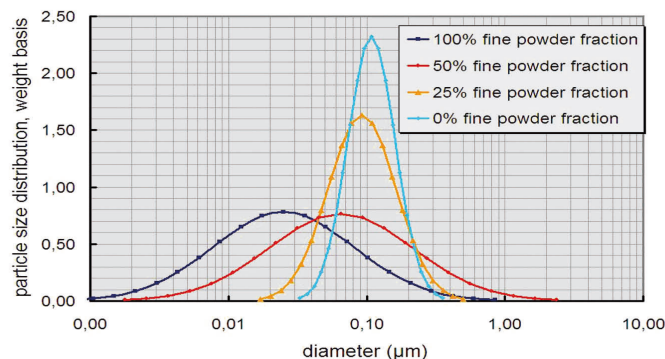


Figure 5.2 Particle size distribution of 20 wt.-% aqueous dispersions containing different mixtures of OX 50 and A 380

## 5.2 Mixtures of powders with different basic raw materials

Mixtures of fine, nanoscaled and coarser, micro scaled powders are often resulting in an undesirable agglomeration of the particles: the finer particles adhere to the surface of the coarser ones.

In the following example an  $\alpha$ -alumina (primary particle size about 130 nm) and a cerium stabilized, tetragonal zirconia (primary particle size about 3,0  $\mu\text{m}$ ) were used. A 20 vol.-% aqueous suspension was prepared from both powders respectively. The systems were stabilized by adding 0,2 wt.-%dwb additive CE64. Furthermore a 1:1 mixture (in wt.-%) was manufactured from both suspensions. The pH was about

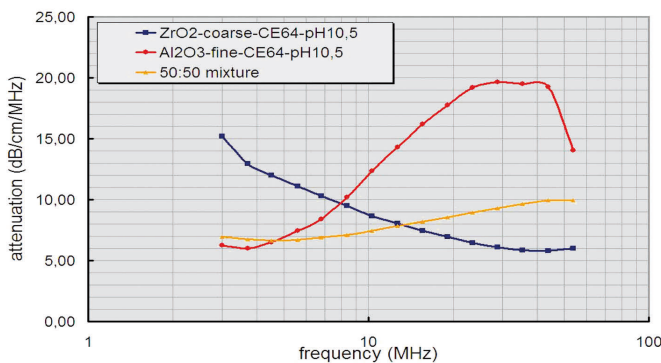


Figure 5.3 Attenuation spectra of the pure zirconia-coarse and  $\text{Al}_2\text{O}_3$ -fine suspensions as well as for the 1:1 mixture; dispersion properties: 20 vol.-% solids content, pH = 10,5, additive fraction (CE64): 0,2 wt.-%dwb

10,5 for all systems. The attenuation spectra of all dispersions are given in figure 5.3.

The alumina shows a characteristic frequency at about 30 MHz, which indicates a submicron size distribution. The characteristic frequency of the zirconia is smaller than 1 MHz – a micro sized powder. In figure 5.4 the analysed particles size distribution can be seen. It is remarkable, that alumina and zirconia can be measured as single modes in the 1:1 mixture – both powders are not agglomerated in the dispersion.

## Conclusion

Powder mixtures can be characterized by means of the DT-1200.

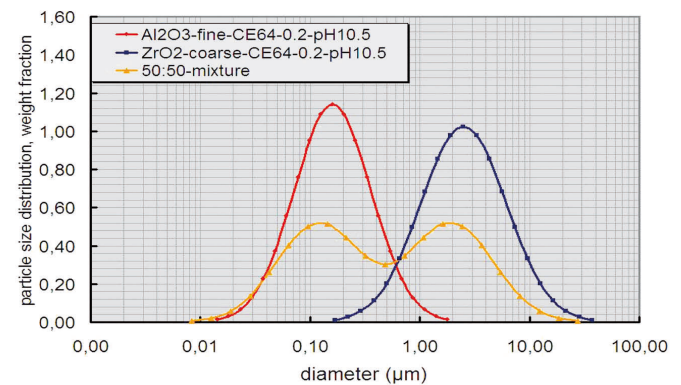


Figure 5.4 The particle size distributions of the three dispersions – analysed from the attenuation spectra of figure 5.3

## 6. Characterization of cement dispersions using ultrasound techniques

By means of ultrasound techniques, important information can be gained regarding the mechanism of the additives' actions in cement slurries as well as the solidification processes. After adding cement to water, two processes are taking place in parallel: firstly ions are dissolved in the water and, secondly, an initial-hydrolysis of calcium-silicate groups occurs: calcium-silica-hydrates (C-S-H-groups) are forming. In the next 4 hours, a steady increase in the rate of hydrolysis takes place: the so called Ettringer Crystallites.

The following analysis was carried out using standard trade cements (CEM I42,5 R and CEM 2925). Further on deionized water was used as dispersing medium (conductivity of 10  $\mu\text{S}/\text{cm}$  maximal). Polycarboxylate-ester, naphthalene sulfonate and a water-soluble copolymer with sulphur groups (FM 2453) acted as dispersants.

The first topic was to investigate the solidification process of the cement dispersions. Additionally the influence of an additive on this process should be tested. In order to do this, a 20 wt.-% cement dispersion (CEM I 42.5) was manufactured – one with and one without an FM 2453 amount of 1 wt.-%dwb. The dispersant was dissolved in water in advance. The dissolving of the cement was done using a commercial laboratory stirrer for 2 minutes. For the measurement of the spectra, both cements were put into the particle size measu-

rement cell of the DT-100, and recirculated using a peristaltic pump.

In figure 6.1 a series of attenuation spectra of the dispersion without the additive is shown in dependence of time. It can be seen from the significant increase of the attenuation in the frequency range higher than 40 MHz, that the hydration is already far proceeded after 5 h. The reason for the increasing attenuation in this range is due to the stronger scattering effect of the coarsening of particles.

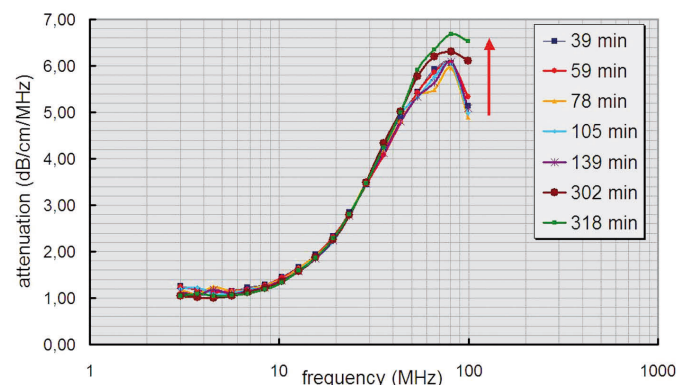


Figure 6.1 Series of measured acoustic attenuation spectra of the 20 wt.-% cement suspension without the additive FM 2453 in dependence on measurement time

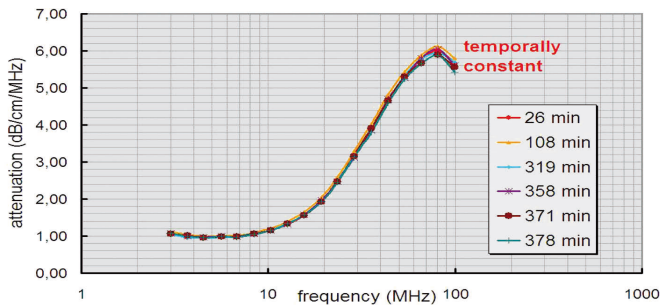


Figure 6.2 Series of measured acoustic attenuation spectra of the 20 wt-% cement suspension with the additive FM 2453 in dependence on measurement time

On the other hand it can be seen in figure 6.2, that the attenuation spectrum of the cement slurry with FM 2453 is not increasing in the upper frequency range even after about 6 h. It seems to be, that the additive delays the solidification process of the cement significantly.

In the second part of this investigation, the influence of the added amount of different additives on the zeta potential of a cement was tested. For dispersions with an extreme high concentration of ions as it is the case for cements, the diffuse layer will be thinned out and sometimes it will collapse normally. This does not happen in the case of hydrophilic surfaces like cements, because the formation of a hydrate-layer displaces the ions in outwards direction and the collapse will be inhibited (figure 6.3). That's the reason why zeta potential can be measured even in case of such systems.

The zeta potential measurements on the cements was carried out using the method of the electroacoustic background: the total measured vibration current (TVI) consists of the fraction of the colloids (colloidal vibration current, CVI) and that of the ions (ionic vibration current, IVI):

$$TVI = CVI + IVI \quad (1)$$

The ionic vibration current is important only in case of a high fraction of the ions in comparison to the colloidal particles. This is the case for dispersions with a high ionic concentration

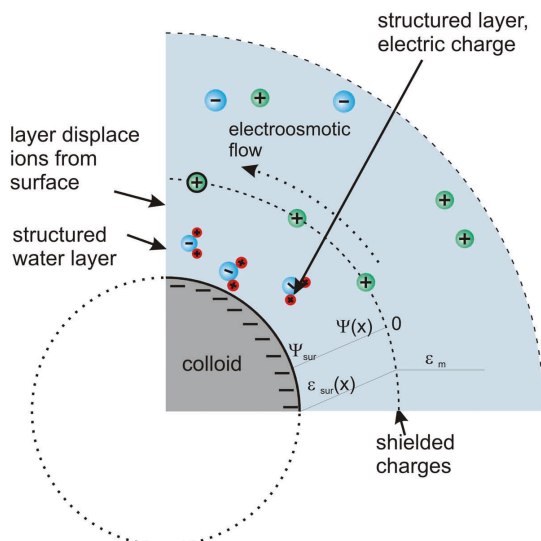


Figure 6.3 Electric double layer for hydrophilic particles in dispersions at a high ionic strength

or with a low particle concentration as well as for dispersions with coarse particles. For cements the reason is the high ionic concentration in water. Figure 6.4 represents the zeta potential of an aqueous CEM 2925 suspension with 66,7 wt.-% solids content (300 ml) in dependence on the added amount of naphthalene sulfonate (ml).

It can be stated, that the higher the zeta potential the more additive will be added. A saturation is reached at about 2 ml additive. Obviously naphthalene sulfonate acts as a electrostatic flux material. In contrast to this the zeta potential of the same cement is decreasing by increasing the amount of polycarboxy-

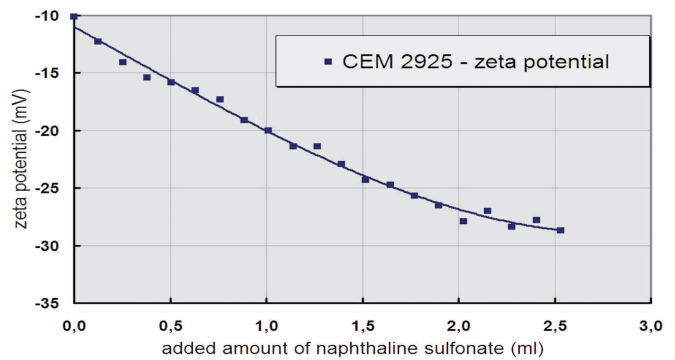


Figure 6.4 Zeta potential of an aqueous cement slurry (66,7 wt.-% CEM 2925) in dependence of the added amount of naphthalene sulfonate

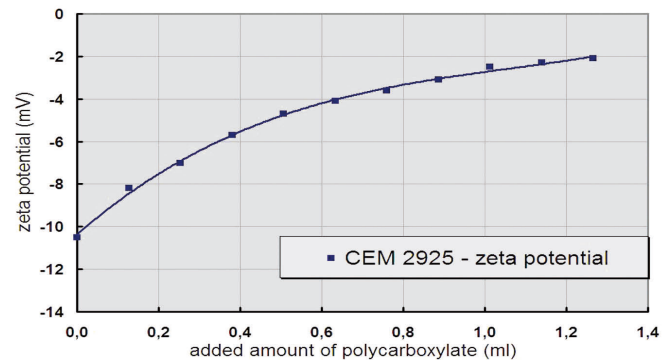


Figure 6.5 Zeta potential of an aqueous cement suspension (66,7 wt.-% CEM 2925) in dependence of the amount of polycarboxylate

late (figure 6.5). Nevertheless this additive decreases the viscosity, it works as a steric additive. The reason for the decrease of the zeta potential is just a shift of the hydrostatic shear layer in case of the adsorption of polymers with longer side chains. If this layer moves outwards, lower zeta potentials will be measured than without adding these adsorbed polymers.

### Conclusion

Acoustic waves are suitable for the investigation of complex, highly concentrated material systems as it was demonstrated for the cement slurries: changes in the acoustic attenuation spectra in dependence of time allows conclusions to be made on the solidification process. The electroacoustic method makes zeta potential measurements possible which can explain the different effects of additives. There are significant advantages of the DT-1200 compared with other techniques: the high sample concentration, the broad particle size range as well as the flexible use of pumps or stirrers distinguish this method from others.

## 7. Rheological analysis of dispersions

The knowledge of rheological properties of dispersions is significant for their manufacturing and processing. In the following example the acoustic rheometer DT-600 was applied for the production and dispersion of an aqueous titanium oxide suspension. The following materials were used for this purpose: titanium oxide „Hombitec“ (primary particle size about 30 nm), deionized water and the additive BYK 190. To investigate the influence of the additive on the rheological properties of the water medium, both, pure water and the water-additive-mixture (10 wt.-%dwb BYK 190) were characterized with the DT-600. In figure 7.1 the measured acoustic attenuation spectra of both liquids can be seen. The attenuation increases significantly by adding the additive. Furthermore a Newtonian test was carried out on the basis of the premise that: the pure water acts as a Newtonian liquid as expected while the mixture is non-Newtonian.

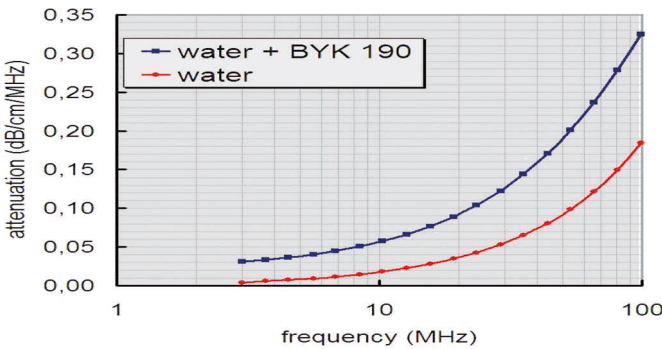


Figure 7.1 Acoustic attenuation spectra of water and water + BYK 190, measured using the acoustic rheometer DT-600

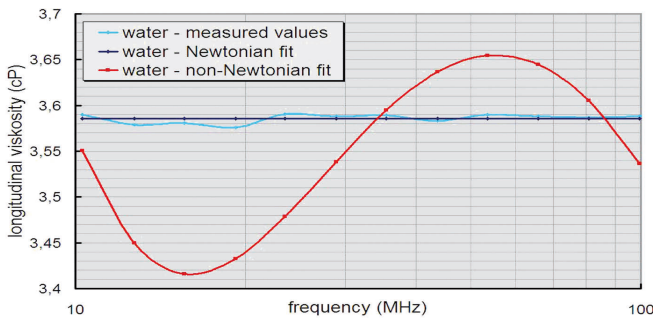


Figure 7.2 Newtonian test with water

Titanium oxide was added to the medium (water + 10 wt.-%dwb BYK 190) in a concentration of 35 wt.-%. This dispersion was characterized by means of the DT-600 (Hombitec-0-sample). The loss module  $M''$  in dependence on the frequency is shown in figure 7.4, the results of the measurement are summarized in table 7.1. It can be seen from the  $M''$  vs. frequency curve, that this dispersion has absolutely non-Newtonian character.

Then the dispersion was milled and dispersed using a laboratory stirring mill (Netzsch LabStar, Zeta Geometry in  $ZrO_2$ , grinding media diameter 0,65 mm YTZ) and measured with the DT-600 regarding its rheological properties. The result was the reduced viscosity due to the milling: the dispersion acts almost as a Newtonian liquid. The milling product was of much lower viscosity. The not dispersed Hombitec-0-sample

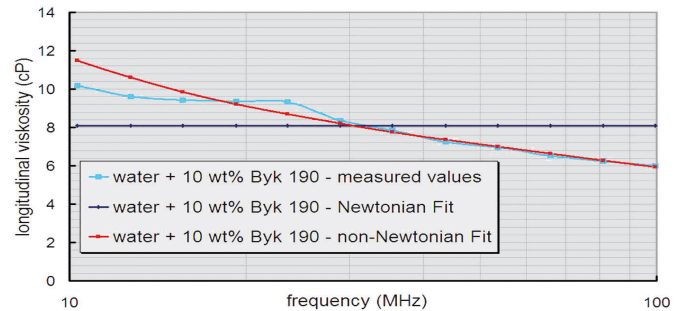


Figure 7.3 Newtonian test with the water + BYK 190 mixture

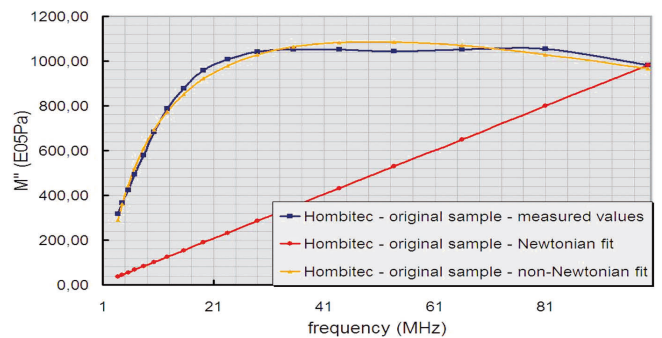


Figure 7.4 Loss modulus  $M''$  of the 0-sample in dependence on the frequency of the ultrasound wave

Name	Temperature (°C)	Dynamic viscosity (cP)	Storage modulus $M'$ E09 (Pa)	Sound speed (m/sec)
water	24	0.91	2.23	1497
water + Byk 190	23	-	2.29	1512
Hombitec – 0-sample	24.5	-	2.9	1452
Hombitec – 90 min milling	24.5	-	2.74	1420

Table 7.1: Collection of the measurement results of the rheological experiment

tended to extreme sedimentation. This is an effect of the stronger agglomeration of the particles, which is resulting in a higher viscosity of this sample.

### Conclusion

By means of the ultrasound spectrometer with rheological option and the DT-600 additional rheological parameters can be investigated and e. g. the Newtonian and Non-Newtonian behaviour of dispersions can be analysed.

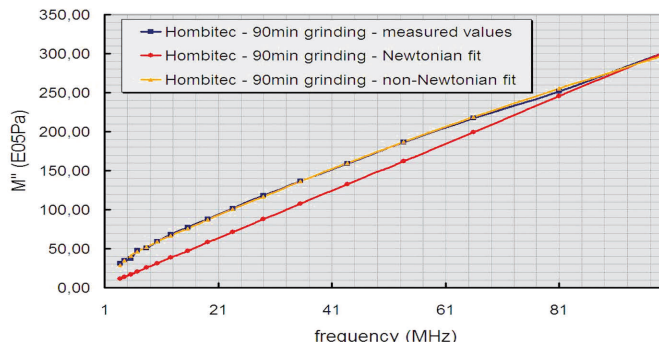


Figure 7.5 Loss modulus  $M''$  of the 90 min milled sample in dependence of the frequency of the ultrasound wave

## 8. Rigid materials in emulsions

Mixtures of emulsions and rigid materials are important for sun creams e.g. In this case it is normally titanium oxide dispersed in a O/W (Oil-in-water)-emulsion. The emulsion guarantees the spreading of the titanium oxide on the skin, while the ceramic powder works as an UV-adsorbing material. Another application is special lubricants. In the following example, a manganese oxide-in-emulsion suspension will be examined using ultrasound techniques. This type of materials is important for lubrication of bore holes. In the first step the O/W-basis emulsion was characterized regarding particle size and viscosity using a DT-100 and DT-600 respectively. The attenuation spectrum of the emulsion in comparison to pure water is presented in figure 8.1. The calculated emulsion drop size is shown in figure 8.2 and the loss modulus  $M''$  can be seen in figure 8.3. Evidently the emulsion shows a Non-Newtonian characteristic.

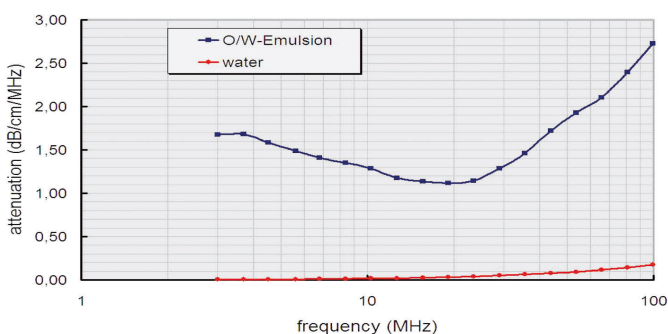


Figure 8.1 Acoustic attenuation spectrum of the O/W-Emulsion and water

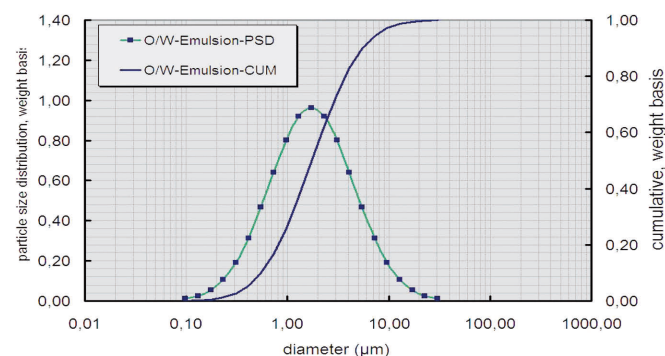


Figure 8.2 Drop size of the oil phase of the O/W-Emulsion

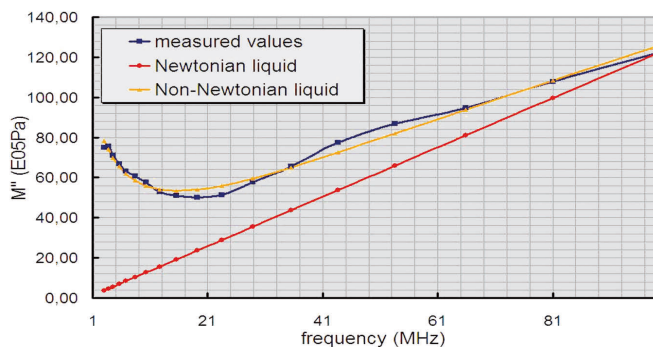


Figure 8.3 Loss modulus of the O/W-Emulsion

The results of the particle size measurements of the O/W-emulsion as well as the manganese oxide dispersion are summarized in table 8.1.

Sample	St.dev.	d10 µm	d16 µm	d50 µm	d84 µm	d90 µm
O/W-emulsion	0.4	0.55	0.715	1.73	4.304	5.437
Manganese oxide-dispersion	0.2	0.766	0.871	1.334	2.073	2.325

Table 8.1: Summary of the particle size distributions

In the emulsion, manganese oxide was dispersed with a concentration of 80 wt.-%. The acoustic attenuation spectra of the complete dispersion as well as for the emulsion (background spectrum) are given in figure 8.4. The calculated particle size of manganese oxide in emulsion is shown in figure 8.5.

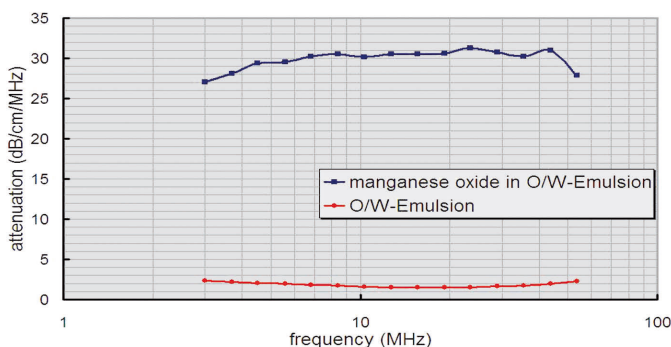


Figure 8.4 Acoustic attenuation spectra of the manganese oxide dispersion in comparison with the pure O/W-emulsion

### Conclusion

Additional rheological investigations can be done by means of the new rheological option of the DT-1200. The combination of the particle size measurement and the analysis of the loss modulus via acoustic attenuation spectrometry can result in gaining additional information about concentrated dispersions.

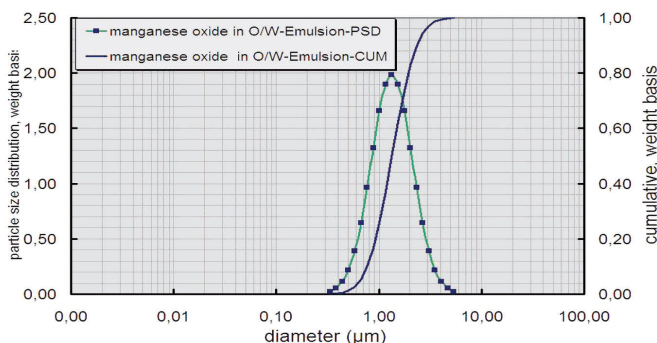


Figure 8.5 Particle size distribution of the manganese oxide dispersion

## 9. Colloidal properties of coarse, „non-colloidal“, highly-dense particles

Colloids are, by definition, particles or droplets with a diameter smaller than 1 µm. For colloids the zeta potential can be a parameter in order to predict stability of the dispersion. On the other hand, this parameter can be an interesting indicator for non-colloidal, coarse particles, for shaping techniques or separation processes e.g.

The problem in measuring zeta potential is the strong tendency to of coarse, highly -dense particles to sediment. That is the reason why only electroacoustic methods are suitable for this application. It should be remembered, that the number of particles, which generate the measurement signal (colloidal vibration current, CVI) are few for such coarse powders in comparison to submicron particles in case of identical absolute weights. Thus the influence of ions on the measurement signal (ionic vibration current, IVI) can modify the calculated result. This is the case especially for a low particle concentration (< 5 wt.-%) in the dispersion. Then the analysis of the zeta potential must be carried out using the method of electroacoustic background.

In this example an aqueous alumina suspension with 20 wt.-% solids content was prepared. The d50 of the powder was about 40 µm. In order to measure the pH-dependency on the zeta potential, HCl and KOH were used. After achieving the desired pH, the suspension was allowed to sediment. Then the ionic vibration current of the clear supernatant was measured and saved as the electroacoustic background. Subsequently, the suspension was stirred and redispersed

and the zeta potential was measured, taking the background into account.

The result of this titration is shown in figure 9.1. The alumina shows the expected progression: it is positive in the acid range and negative in the basic one. The isoelectric point (IEP) is located at about 9,3.

### Conclusion

The measurement of zeta potential with the DT-1200 and DT-300 is possible also in case of coarse particles, if the so-called background method is applied if necessary.

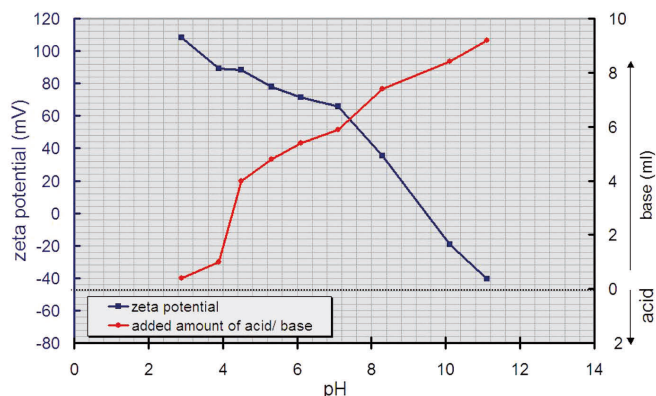


Figure 9.1 Zeta potential's dependence on the pH of the 20 wt.-% alumina suspension, measured via the method of the electroacoustic background

## Near-process particle size measurement using the acoustic spectrometers DT-100 and DT-1200

### Introduction and motivation

For many applications, the knowledge of the primary particle size of a basic powder is important. An example is the processing of ceramic powders, where the pore structure and density and thus the sintering behaviour of the green bodies depends directly on the particle size distribution. In the construction industry, the solidification process and processability of cements is a function of this parameter. Another example is the food industry, where the quality of chocolate depends strongly on the particle size of the choco-



late powder. The knowledge of the real particle size or, in other words, the state of dispersion, is often much more important for the quality of a dispersion than the primary particle size: the state of dispersion determines the properties like processing, storage stability and the quality of the final product. Established optical methods like laser diffraction cannot fulfil this function, because they are limited to strongly diluted systems. In the real application, the concentration of the dispersions is normally much higher than 1 % and a dilution usually changes the properties of the system.

For this reason the techniques based on ultrasound are becoming more and more established. Because of different physical properties in comparison to optical waves, dispersions with a concentration up to 60 vol.-% can be analysed via ultrasound waves. For many applications like functional layers or silica gels, nanoscaled particles (mean particle size of 5 – 100 nm) play an important role. Modern ultrasound spectrometers are able to characterize nano-particles in a large size- and concentration-range.

In this article, the operating mode of the ultrasound spectrometer DT-100 will be discussed. After the description of the principles of the measurement, some physical and colloidal-chemical basics of the acoustic spectrometry will be presented.

### Ultrasound spectrometry – principle of measurement

A sound transducer transforms a high-frequency signal into an ultrasound wave (figure 1). This wave will be launched into the dispersion to be characterized. During transmittance of the wave through the dispersion, it will be attenuated due to different mechanisms (see below). The attenuated signal will be detected by the sound receiving transducer and forwarded to the computer for signal-conditioning and analysis. Apart from the specific effects in the dispersion ( $I_0$  to  $I$ ), the attenuation is dependant on the gap  $L$  between sender and detector as well as on the sound frequency  $f$ :

$$\text{attenuation}(\text{dB/cm/MHz}) = \frac{10}{fL} \log\left(\frac{I_0}{I}\right) \quad (1)$$

The dependency of the attenuation on sound frequency can be used to analyse the particle size distribution in the dispersion. The decisive question is, how does the measured attenuation spectrum depend on the particle size distribution, and which mechanisms are responsible for the attenuation of the incoming wave (intensity  $I_0$ ) to the outgoing wave ( $I$ ) at the particular wave length.

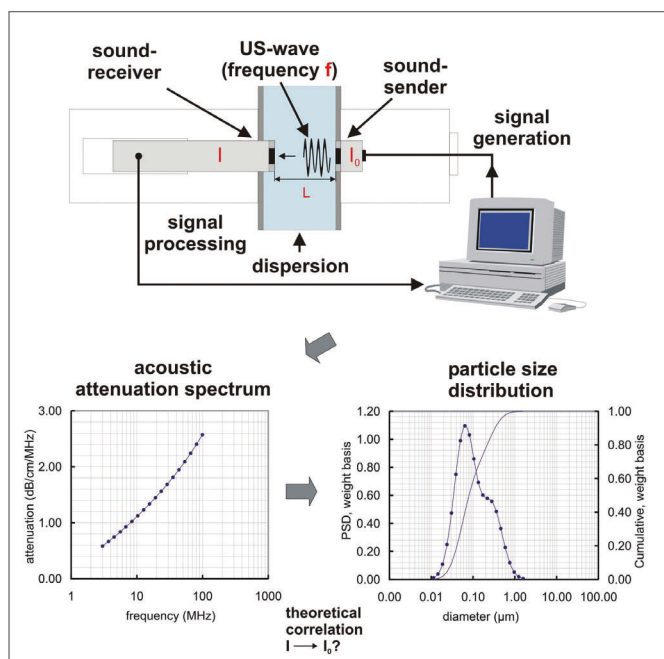


Figure 1 Measurement principles of the ultrasound spectrometry

### Ultrasound in liquid dispersions – absorbing mechanisms and their modelling

A dispersion is generally a substance (disperse phase) distributed in a dispersing medium (continuous phase). In case of liquid dispersions, the continuous phase is a liquid. For a solid, disperse phase, it is called a suspension, a liquid-liquid dispersion is an emulsion. A foam means a liquid dispersion with a gaseous dispersed phase.

An ultrasound wave, which is transmitting through a liquid dispersion, will be attenuated with the increasing path length. Basically, there are three effects responsible for this:

1. intrinsic absorption
2. dissipative absorption and
3. sound scattering.

#### 1. Intrinsic absorption:

is the attenuation of the sound wave of the continuous as well as of the dispersed phase of the dispersion. In solids, that are the rigid particles of a dispersion, the attenuation is relatively small and can be neglected for the acoustic attenuation. In pure liquids, the sound wave will be predominantly attenuated due to the formation of compacted and expanded areas, which results in temperature gradients and pressure relaxation processes. These effects are energy intensive (figure 2). In case of coarser molecules, relaxation effects like rearrangements of molecules can be responsible for an additional attenuation of the sound wave.

Examples for intrinsic attenuation spectra of pure liquids are shown in figure 3. Two different types of liquids can be distinguished: Newtonian and non-Newtonian liquids. In case of Newtonian liquids, the attenuation shows a linear dependency on the frequency. This is the case for water or cyclohexane respectively. Glycerine or propylene-glycol 400 on the other hand are examples of non-Newtonian liquids.

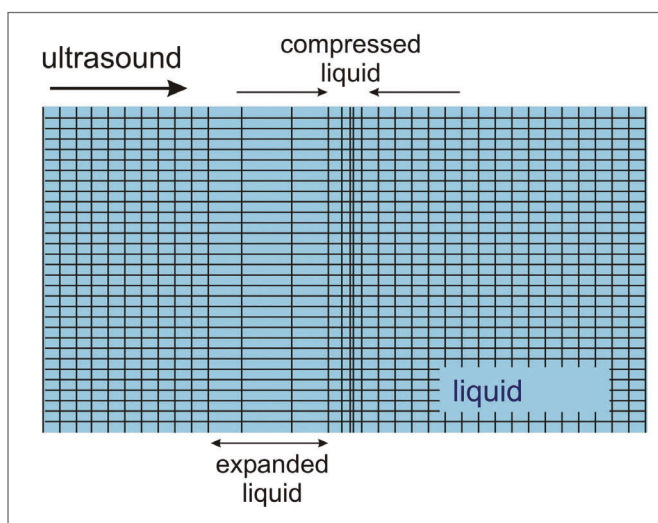


Figure 2 Effect of the ultrasound wave in a pure liquid – formation of expanded and compacted areas

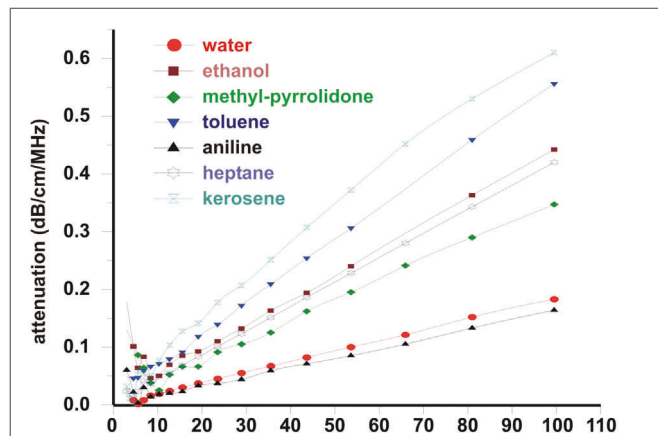


Figure 3 Ultrasound attenuation spectra of pure liquids

#### 2. dissipative absorption:

this is the ultrasound attenuation due to dissipative interactions between continuous and dispersed phase. Dissipative means, that a system is losing energy, which will be transformed into thermal energy. In principle three different effects can be distinguished, which will be described below.

##### 2.1 viscous-inertial effect:

this is a hydrodynamic mechanism and it will increase with an increasing density contrast (difference in density) between the dispersed phase and the medium. During the transmission of the wave through the dispersion, the density contrast causes a relative movement of the particles to the continuous phase. This leads to a shearing of the liquid layers at the liquid-solid interphase: the wave will be attenuated due to shear friction (figure 4). This effect is predominant for suspensions with rigid, coarse particles smaller than about 4 µm (ceramics, pigments, ...).

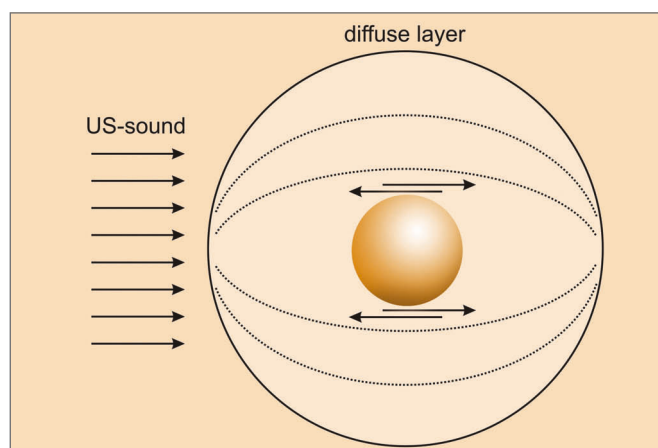


Figure 4 Mechanism of the viscous-inertial effect

Examples of the viscous-inertial effect are given in figure 5. The graph shows several attenuation spectra of an aqueous model suspension with a solids content of 20 vol.-% and a particle density of 3 g/cm<sup>3</sup>. The effect of the particle size on the curve progression and shape is shown. It can be seen in the figure, that for this effect, the curves of the mean sizes (0,4 and 0,8 µm) are showing a maximum at a characteristic



frequency. Generally, this characteristic frequency is increasing with a decreasing particle size. The following equation is valid for most cases

$$f_{cr} \approx \frac{\eta}{\rho d^2} \quad (2)$$

For 3,0  $\mu\text{m}$  particles, the maximum is located at a lower frequency than the presented range, which means lower than 1 MHz. In case of the 0,2-, 0,1 and 0,05  $\mu\text{m}$  suspension, the characteristic frequency is higher than 100 MHz.

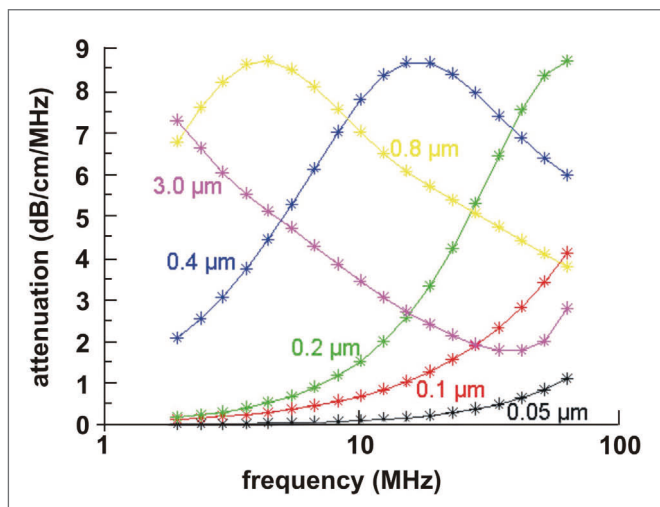


Figure 5 Viscous-inertial effect of different aqueous model suspensions with a solids content of 20 vol.-% (density 3 g/cm<sup>3</sup>)

The experimental description of the viscous effects started already in the 1940th with the works of Urick [1] and Ament [2]. The model of Ament pointed out, that the individual phases can appear with certain amounts and it provided a possibility to take several different dispersed phases into account. The most common acoustic theory is surely the ECAH theory, which was developed by Epstein, Carhart, Allegra and Hawley [3-4]. It is applicable only for diluted systems and describes the viscous as well as the thermal attenuation mechanism. The theory integrated in the DT-100 to model the viscous-inertial effect is the so-called advanced coupled phase model (PKM) developed by Dukhin and Goetz [5-6].

## 2.2 thermal effects:

the nature of this mechanism is thermodynamical. The transmitting ultrasound wave leads to pressure- and density-fluctuations in the dispersed- as well as in the continuous phase. The consequence is the appearance of different temperature fluctuations inside the phases due to the thermodynamical coupling of pressure and temperature. These fluctuations lead to the formation of temperature gradients at the phase boundary (figure 6). The temperature compensation results in an increase of the oscillation energy. This effect is dominant for emulsions and plays a role in e.g. latices as well. For aqueous suspensions, it is normally negligible.

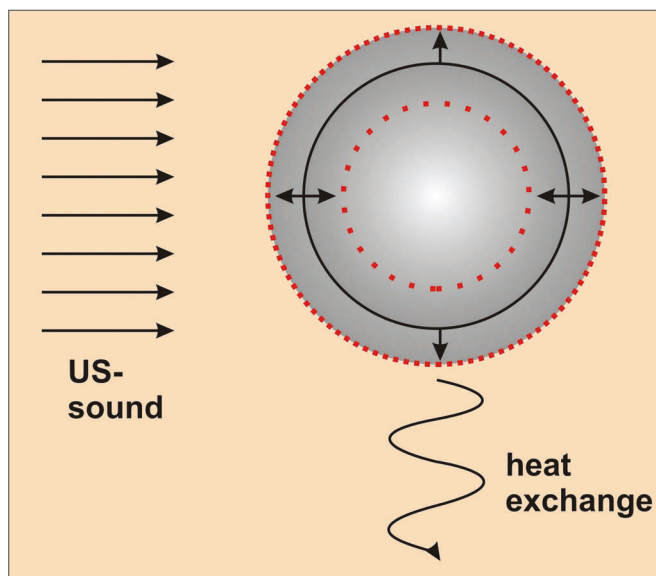


Figure 6 Thermal effects

The thermal effects in a latex suspension (mean particle size of 160 nm) can be seen in figure 7. The attenuation of the suspension is shown versus the latex weight fraction.

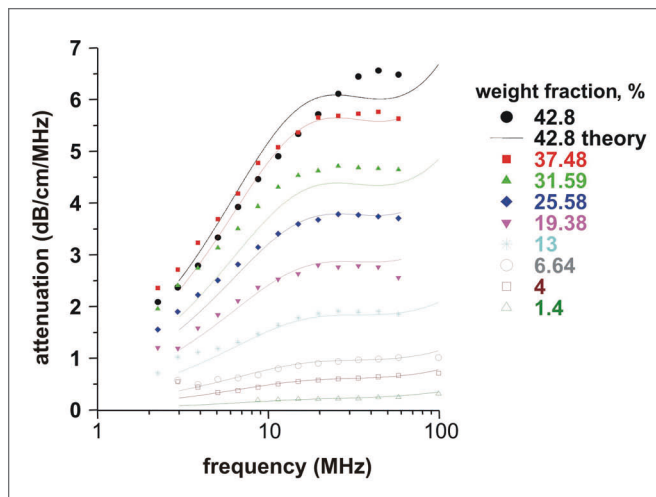


Figure 7 Thermal effects in a latex suspension at different latex contents, mean particle size is 160 nm

If one compares the 19,38 vol.-% latex suspension with the 0,2  $\mu\text{m}$  model suspension (figure 5), it can be seen, that the viscous attenuation is clearly stronger than the thermal one (about 3 dB/cm/MHz maximal attenuation for the emulsion and 9 dB/cm/MHz for the suspension).

To focus on the history of the modelling of the thermal effects it is necessary to reach once again for the ECAH theory. The theory which is integrated in the DT-100 for the description of this effect is the model of the „particle-medium-coupling“ (PMK) of Isakovitch [7].

### 2.3 Structural effects:

this attenuation mechanism appears in structured dispersion (highly concentrated dispersions or systems with binders). The individual mobility of a particle in the continuous phase is strongly influenced by the others. Such structured systems have dissipative as well as elastic properties. For this case one can imagine the particles as interconnected by springs (figure 8, Rouse-Bueche-Zimm model, integrated in the DT-100 [8]). The springs are representing the elastic fraction. The viscous fraction of the particles moving through the liquid is represented by the attenuation module. It is inversely proportional to the Stokes resistance value. This additional energy loss can be determined by means of the Hooke's law:

$$F = X\Delta X + \delta \frac{\Delta X}{\Delta t} \quad (3)$$

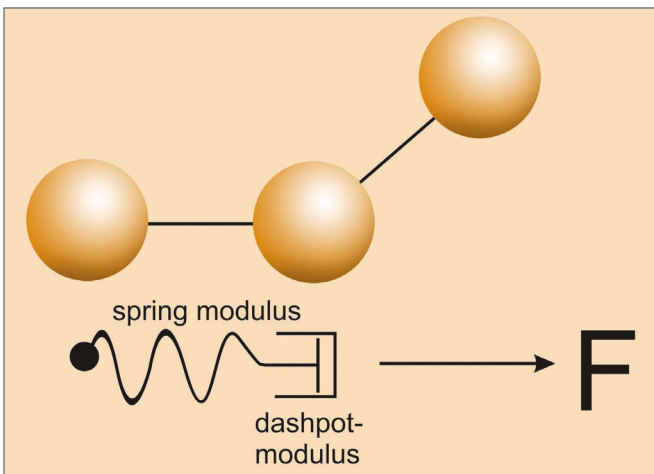


Figure 8 Structural losses

According to the theory it can be concluded, that the relevant mechanism for sound attenuation is the dissipative fraction here. This can be seen clearly from figure 9: the left image shows the influence of the Hooke elasticity coefficient on the attenuation of a 40 vol.-% alumina suspension ( $d_{50} = 1 \mu\text{m}$ ).

Apparently the shape of the curve is independent of this parameter, just the attenuation maximum is shifted to higher frequencies. The right graph shows the influence of the Hooke loss coefficient on the attenuation spectrum of this dispersion. In this case the shape of the curve is changing significantly – the parameter is used as an additional fit parameter.

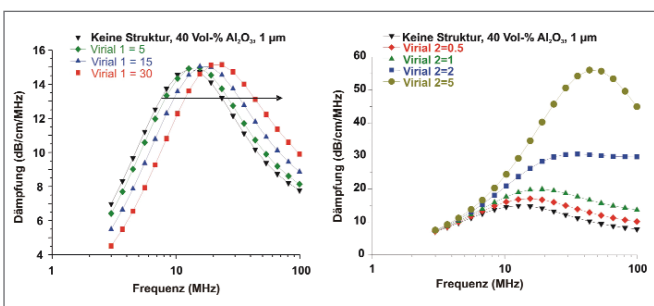


Figure 9 Structural effects at a 40 vol.-%  $\text{Al}_2\text{O}_3$ -suspension ( $d_{50} = 1 \mu\text{m}$ ), left: the Hooke elasticity coefficient (virial 1); right: the Hooke loss coefficient (virial 2)

### 3. sound scattering:

Scattering of sound waves at meeting particles in a dispersion is similar to light scattering. This is not a dissipative effect, but the sound wave will be partially deflected in other directions in space. The total energy will be conserved (figure 10). Effects, which play a role, are reflection and refraction at the phase-boundaries as well as diffraction directly at the particle itself. The scattering effect is only important in the so called long wave regime. This means that the wave length of the ultrasound wave is much bigger than the particle size diameter. For ultrasound spectrometry, this is the case for particles bigger than about  $5 \mu\text{m}$ .

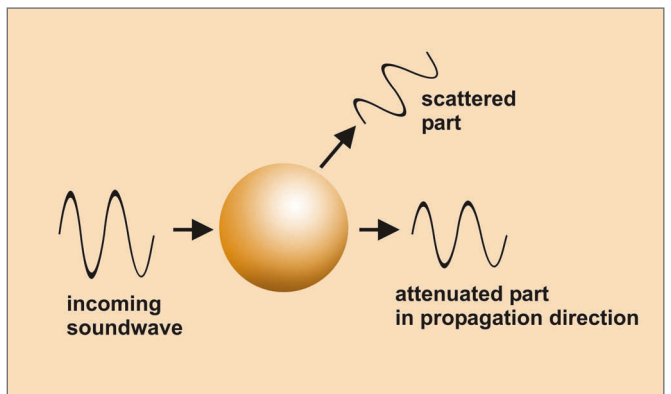


Figure 10 Sound scattering

The first approaches to describe sound scattering at an individual particle can be found in a paper of Rayleigh in 1880. The ECAH-Theory on the other hand describes the scattering for diluted systems. The model for concentrated dispersions, which is integrated in the DT-100, is a modification of the Morse theory [9]. The intrinsic and the dissipative effects as well as the sound scattering are independent from each other. The acoustic approach of superposition [6] says, that the total acoustic attenuation  $\cdot T$  of an acoustic wave in a dispersion can be written by the sum of all individual attenuation mechanism:

$$\alpha_T = \alpha_{int} + \alpha_{vis} + \alpha_{th} + \alpha_{st} + \alpha_{sc} \quad (4)$$

Figure 11 demonstrates the superposition approach in a diagram: the measured spectrum (black curve) is an overlay of all mechanisms 1 to 5. The intrinsic loss in the pure solvent is independent of the particle size and will be subtracted from the total spectrum as a background. The remaining spectrum consists now just of the particle size depending mechanisms 1 to 4. On the basis of the specific theory for each mechanism integrated in the software, this remaining spectrum will be fitted in and the particle size will be calculated from this.

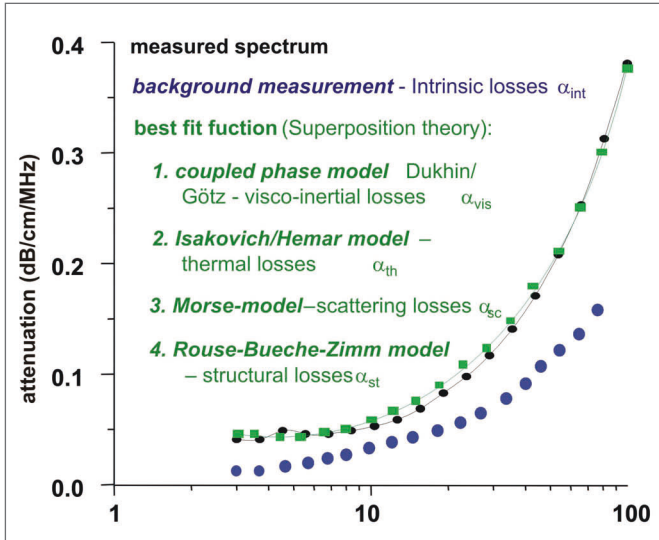


Figure 11 Principle of superposition demonstrated in a diagram

**Technical performance:  
the ultrasound spectrometer DT-100**

The dispersion to be characterized will be poured into the measurement chamber of the DT-100 (figure 12). In addition to the acoustic sensor, probes to measure the pH, temperature, conductivity and zeta potential can be incorporated. Furthermore, the titrator can be used for a software controlled automatic measurement in dependence on the pH or the amount of an additive respectively.

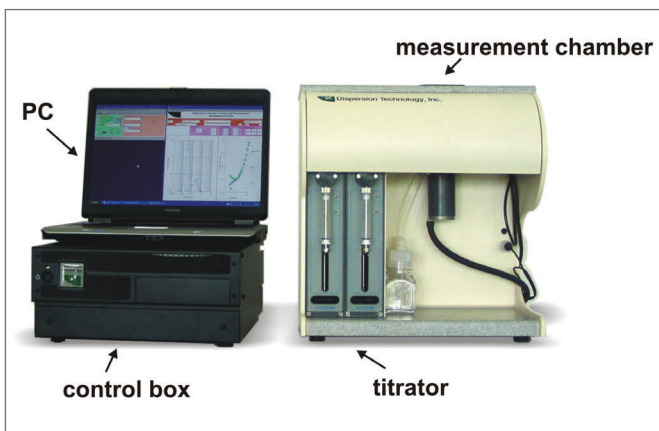


Figure 12 Ultrasound spectrometer DT-100

A high frequency signal will be sent from the controller box, which will be transferred from the deep-seated sender into an ultrasound wave by means of a piezo transducer. This wave will enter the dispersion that is present in the measurement chamber. This chamber is made of Kynar, a very resistant polymer. The wave will be attenuated in the dispersion, the signal will be detected by the receiver at the opposite ultrasound transducer and used for the particle size analysis. The principle of measurement is the so called „tone-burst“-method: short wave packets with a very narrow frequency

distribution and a few numbers of oscillation cycles are sent through the dispersion chamber (figure 13, filled with the dispersion). Sound attenuation and -speed are measured by detecting signal attenuation and -delay. The gap between sound-sender and -detector is variable: thus a bigger range of dispersion-concentration can be characterized. At smaller gaps, the higher concentrated systems shows a much better signal to noise ratio, while more diluted dispersions attenuate adequately only at bigger gaps and can be measured therefore only under these conditions.

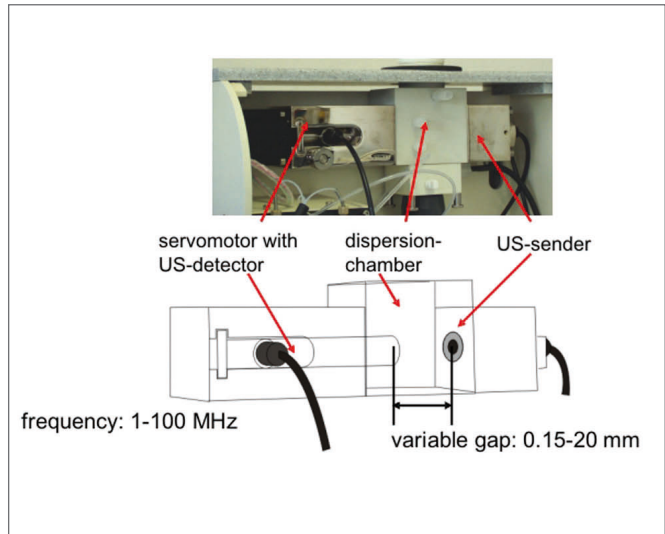


Figure 13 Acoustic measurement block for particle size analysis

The frequency range of the DT-100 is 1-100 MHz. The gap between sender and detector is variable from 0,1 to 21 mm. During the measurement process, at least 800 signals for each gap and frequency will be detected and averaged. The signal to noise ratio of every measurement can be monitored online (figure 14).

The measurement can be carried out in static as well as in flow conditions.

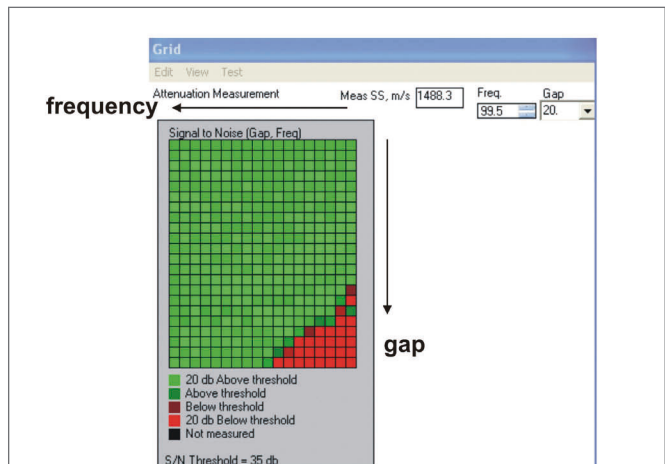


Figure 14 Example of an online-monitoring of the signal to noise ratio of all the measuring points in an acoustic attenuation measurement

### Particle size measuring process using DT-100

Before starting particle size measurement using the ultrasound spectrometer DT-100, we need to define the phases of the dispersion ("1" and "2" in figure 15). The required parameters must be put into the Microsoft Access database. Then they can be used every time for subsequent measurements. Each phase (liquid or solid) must be defined just once. Depending on the type of dispersion (suspension or emulsion), different parameters must be known.

In case of a suspension with rigid particles, one needs to know just the density of the liquid ("3" in figure 15). For an emulsion, the thermal expansion coefficient for the liquid is required, but it can be calculated as well from the fit procedure. The parameters "viscosity" and "intrinsic attenuation" of the liquid can be measured using the instrument, if they are not already saved in the data base. For the definition of the dispersed phase(s), the knowledge of the density and ("4" in figure 15) the concentration ("5" in figure 15 in weight-%, volume-% or absolute numbers) is necessary. For emulsions the thermal expansion coefficient of the dispersed phase should be known or calculated during the measurement. It's beneficial to distinguish in advance between coarse ( $d_{50} > 5 \mu\text{m}$ ) and fine ( $d_{50} < 5 \mu\text{m}$ ) powders. This can often be estimated by a visual observation of the sedimentation behaviour.

After measuring the acoustic attenuation spectrum the theoretical fit-spectrum will be automatically adapted to the measured spectrum. The particle size distribution is based on the calculated best fit-parameters. The used model for the calculation or the combination of the models depends on the type of the dispersed phase(s):

1. For fine particles ( $< 5 \mu\text{m}$ ) just the dissipative mechanism is important. In case of rigid particles (ceramics, metals e.g.), only the visco-inertial effect will be considered. For soft particles, thermal effects must be taken into account and for emulsions, only the thermal attenuation mechanism is effective.

2. for coarse particles ( $> 5 \mu\text{m}$ ) additionally the scattering losses must be considered.

3. Structural effects will be taken into account for highly concentrated dispersions or systems with a higher content of binder. This dispersion-characteristic can be estimated from the measured sound speed: if this measured speed is essentially bigger than the theoretically calculated sound speed, the systems show structural effects. In this case the particles are in contact or cross linked, and conducting the sound much faster than isolated particles.

### Conclusions

The modern ultrasound spectrometry enables the particle size distribution measurement in concentrated dispersions. Thus a near process characterization is possible. For a correct analysis the knowledge of the amount of the dispersed phase(s) is required. Furthermore one needs to know the density contrast between the continuous and the dispersed phase in case of suspensions. For emulsions, the knowledge of the thermal expansion coefficient is helpful. The ultrasound spectrometers DT-100 and DT-1200 are measuring the acoustic attenuation in a frequency range of 1 to 100 MHz at a variable sender-detector gap. It allows the determination of particle sizes in the range of 5 nm to 1000  $\mu\text{m}$  at a concentration range of 0,1 to 50 vol.-%, if modern theories are integrated.

### Literature

[1] Urlick, R.J., „The absorption of sound in Suspensions of irregular Particles“, *J. Acoust. Soc. Am.* 20, 3, 283-289 (1948).  
 [2] Arment, W.S., „Sound propagation in Gross mixtures“, *J. Acoust. Soc. Am.* 25, 641-683 (1953).  
 [3] Allegra, J.R., Hawley, S.A., „Attenuation of Sound in Suspensions and Emulsion: Theory and Experiments“, *J. Acoust. Soc. Am.* 51, 1545-64 (1972).  
 [4] Epstein, P.S., „On the Absorption of sound by suspension and emulsions“, in *Applied Mechanics (Th. Von Karman Anniversary Volume)*, 162-188 (1941).  
 [5] Dukhin, A. S.; Goetz, P. J., *Langmuir* (1996), 12, 4336-4344.  
 [6] Dukhin, A. S.; Goetz, P. J., *Ultrasound for Characterizing Colloids - Particle Sizing, Zeta Potential, Rheology*; Elsevier: Amsterdam, (2002).  
 [7] Isakovich, M.A., *Zh. Experm. I Teor. Fiz.* 18, 907, (1948).  
 [8] Mason, W.P., „Dispersion and Absorption of sound in high polymers“, in *Handbuch der Physik, vol.2, Acoustica, part 1* (1968).  
 [9] Morse, P.M., Uno Ingard, K., „*Theoretical Acoustics*“, 1968 McGraw-Hill, NY Princeton University Press, NJ, 925 p (1986).

Content				Density	SSpeed
%wt	%vl	gm	ml		
90.	95.21	99.7	100.	.997	1497.
10.	4.79	11.08	5.04	2.2	5900.
				1.055	1490.6

Figure 15 Input parameters in the particle size measurement experiment on a Silica Ludox suspension using DT-100

## Near-process measurement of colloidal properties (zeta potential) by means of the electroacoustic devices DT-300 and DT-1200.

### Introduction and applications

A comprehensive knowledge of the colloidal properties of liquid dispersions is essential for many applications in the basic- and applied research as well as for industrial processes. Zeta potential, dynamic mobility or Debye-length are important parameters for all procedures related to the movement of colloidal particles in electric fields. Separation processes in the medicinal technology, coating and shaping technologies in the metal- and ceramic industry are examples. On the other hand, the stability of a dispersion against sedimentation, agglomeration or creaming as well as flowability and processability are intimately connected with these parameters.

In case of optical methods like micro electrophoresis or laser-doppler method, a strong dilution of the dispersion is necessary, as a result this characterization is not process-oriented, on the other hand the surface potentials are strongly dependent on the surrounding medium. The dilution will modify the ambience of the particles. Furthermore, in case of high density particles, sedimentation of particles can disturb the electrophoretic measurement as well as fluid flows in systems with a high electric conductivity. In contrast to that, a near-process characterization of the concentrated original sample can be analysed using the electroacoustic method. Furthermore surface- and mass-specific titration experiments can be carried out due to the known solid content.

We shall start with the basic theory of colloidal chemistry followed by the application of electroacoustic methods for the determination of colloidal parameters.

### Colloidal parameters

According to the Stern double layer model, colloidal particles form a strong adherent charge layer (Stern layer) at the surface (figure 1). The colloidal properties of a particle in a dispersion can be divided into two groups: the properties in a steady state and those in motion.

If one takes a look at the Stern double layer model in figure 1 for a particle in a steady state, two colloidal parameters are important for the characterization: the Stern potential  $\Psi_D$  and the Debye length  $\kappa^{-1}$ . Taking into account the Boltzmann statistic and the Poisson equation, it follows for the ionic distribution  $\kappa^2$  around a charged particle [1]:

$$\kappa^2 = F^2 \sum_i \frac{c_i z_i}{\varepsilon_0 \varepsilon_m RT} \quad (1)$$

The Debye length is calculated from the reciprocal square root of this ionic distribution and correlates with the thickness of the diffuse double layer. In equation (1),  $c_i$  indicates the

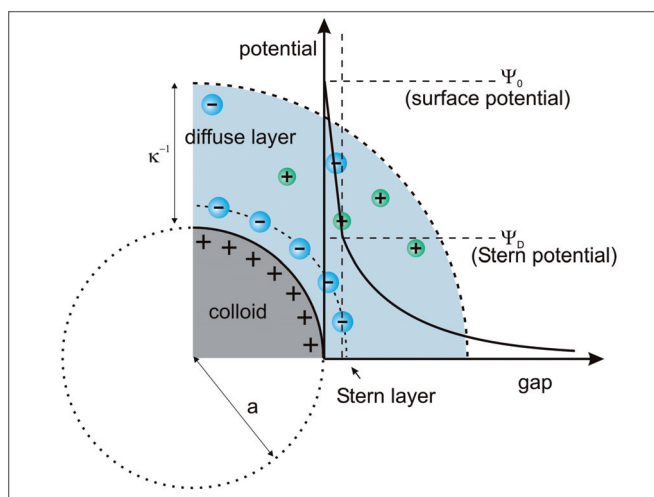


Figure 1 Stern double layer model for a colloidal particle in steady state

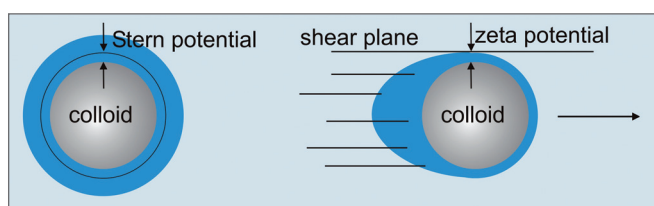


Figure 2 Colloidal particle in steady state and in motion

electrolyte concentration,  $z_i$  the ionic valence,  $\varepsilon_0$  and  $\varepsilon_m$  the dielectric constant and permittivity,  $F$  the Faraday constant,  $R$  the gas constant and  $T$  the absolute temperature. In the literature, the  $ka$ -value is a common parameter: it is the product of the particle size and the reciprocal Debye length. This value represents the relation between double layer size and particle radius. The Stern potential  $\Psi_D$  is a theoretical construct and cannot be measured. It is approximately in accordance with the zeta potential (see below).

Two parameters are particularly interesting for a moving particle: the zeta potential  $\zeta$  and the particle speed  $v$ . The zeta potential (figure 2) is defined for a particle in motion as follows: it is the potential difference between the layer of the sheared diffuse cloud and the pure dispersion medium. The particle speed is always depending on the applied electric field, which is responsible for the motion of the particle. For comparison reasons, the parameter „mobility“  $\mu$  is normally used. For a moving particle in an electric d.c. field,  $\mu$  is defined as

$$\mu = \frac{v}{E} \quad (2)$$

In case of the electroacoustics, an alternating field, the acoustic wave, is responsible for an alternating movement of the particle: thus the parameter „dynamic mobility“  $\mu_D$  is used.

## Determination of colloidal properties from the colloidal vibration current

### Electroacoustic measurement – principles of the technique

The principle of the electroacoustic measurement is shown in figure 3. A high frequency signal (RF-pulse) is transferred into an ultrasound wave by means of a piezo transducer. This wave passes a quartz delay rod, then a buffer rod and will be launched into the dispersion as a narrow frequency, short pulse. The colloidal particles in the dispersion will start a frequent motion relative to the surrounding liquid because of their mass inertia. Thus the particles are shifted relative to their diffuse double layer: short time dipoles are generated, which induces a measurable, alternating current - the colloidal vibration current (CVI). This will be measured as a potential between two electrodes and it will be used to determine the colloidal properties of the sample.

Below the theoretical correlation between the measurement parameters „CVI“ and „electric conductivity“ and the calculated parameters „zeta potential“, „dynamic mobility“ and „double layer thickness“ will be discussed.

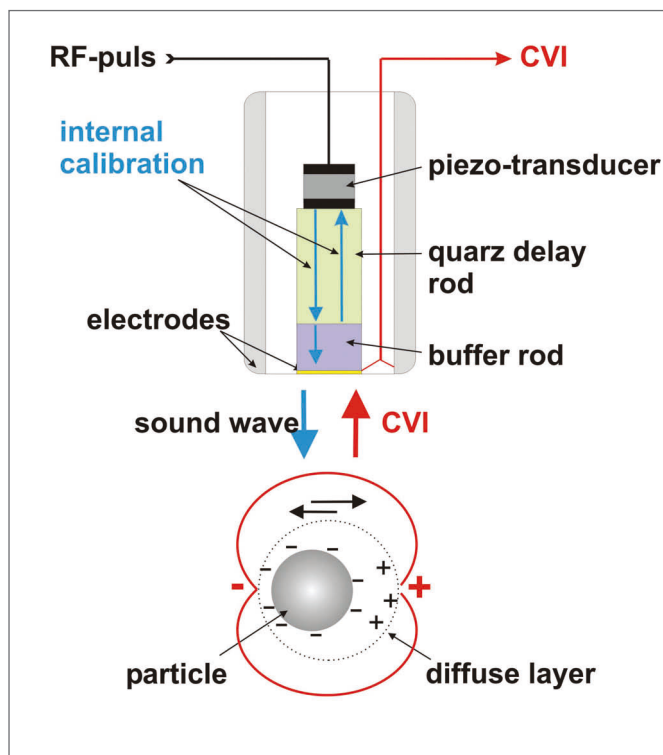


Figure 3 Electroacoustic measurement principle

### Electroacoustic theories

Already in the year 1933 Debye found, that acoustic waves can generate alternating potentials between different areas in solutions of electrolytes due to different ion-masses – friction coefficients. This led to measurable electric currents. This phenomenon is described as the ion vibration potential (IVP). A similar effect was observed for the first time for colloidal dispersions in 1938 by Hermans and Rutgers [4] and presented in a theory by Enderby and Booth [5] in 1951: the colloidal vibration potential (CVP). The problem here was the complexity of this approach and its limitation to diluted systems. There were some scientific papers published between 1960 and 1980, based on the original theory of Enderby and Booth. In the eighties, the inverse effect, the electro sonic amplitude (ESA) was described for the first time. It was the aim of these papers to simplify the complex approach of Enderby and Booth and expand the theory to concentrated systems. The most important publications were the works of Marlow, Fairhurst and Pendse [6]. They applied a cell model (Levine cell model [7]) to the electroacoustics to expand the Enderby-Booth-theory to concentrated dispersions. But this theory was mathematically too complex. An alternative way was described by O'Brien in 1988 [8]: he postulated a correlation between the dynamic mobility (the equivalent to the mobility or electrophoretic mobility in an alternating field) and the measurable, electroacoustic parameters (ESA and CVP or CVI respectively, CVI = colloidal vibration current). He also extended his theory to concentrated systems.

In 1999, an international group of researchers (Shilov (Ukraine), Ohshima (Japan), Goetz (USA) and Dukhin (USA)) significantly advanced the theory of Enderby and Booth. An important development was the introduction of an electroacoustic equivalent to the electrokinetic theory (Smoluchowski [9]), which describes the electrophoretic mobility of colloidal particles: Smoluchowski dynamic electroacoustic limit (SDEL-theory) [10-11]. This one will be described below.

### The SDEL-theory

The SDEL-theory is valid just for low frequencies. The reason for this is, that the basis of this theory is an equilibrium relation of different, thermodynamic variables, which is only valid in a quasi-stationary field, that is at low frequencies (Onsager relation [12]). In figure 4 this approach is demonstrated: the incoming ultrasound wave creates a pressure gradient  $\nabla P$ , which shifts the liquid relative to the particle – a colloidal vibration potential CVP is generated. Beside this effect, an electro-osmotic current  $\langle I \rangle$  as well as an electro-osmotic flow  $\langle V \rangle$  occur. According to Onsager relation, the quotient of CVP and  $\nabla P$  on one side and  $\langle V \rangle$  and  $\langle I \rangle$  on the other side are in an equilibrium.

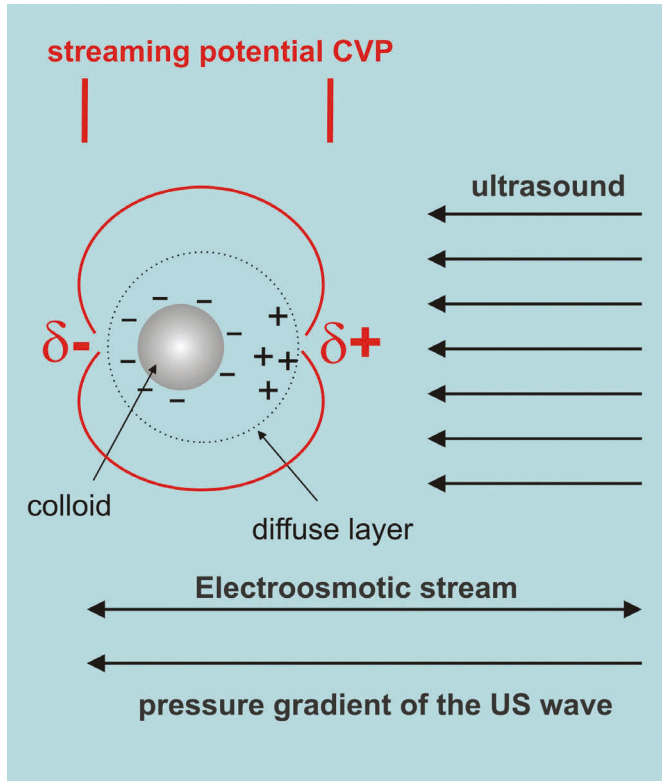


Figure 4 Approach to the SDEL-theory according to Onsager

Considering the above and taking into account the Smoluchowski relation for electrophoresis, the SDEL-theory results in:

$$\frac{CVI_{\omega \rightarrow 0}}{\nabla P} = \frac{\epsilon_m \epsilon_0 \zeta \varphi K_s (\rho_p - \rho_s)}{\eta K_m \rho_s} \quad \text{and (3)}$$

$$\mu_d = \frac{\epsilon_m \epsilon_0 \zeta K_s (\rho_p - \rho_s) \rho_m}{\eta K_m (\rho_p - \rho_m) \rho_s} \quad (4)$$

Thereby  $\epsilon_0$  and  $\epsilon_m$  are the dielectric constant and permittivity,  $\zeta$  is the zeta potential,  $\rho$  is the density with the index  $\pi$  for particle,  $\sigma$  for dispersion and  $m$  for medium.  $K$  stands for the electric conductivity (same index meanings),  $j$  is the volume fraction and  $\tilde{E}$  is the intrinsic viscosity.

The SDEL-theory is valid for any particle concentration and a thin double layer ( $\kappa a \gg 1$ ). But, the surface conductivity must be negligible ( $Du \ll 1$ ). This limitations of the SDEL-theory for the application led to the development of a more generally applicable theory, which was created by the above mentioned group of researchers.

### The advanced CVI-theory

The advanced CVI-theory as integrated in the DT-300 consists of a solution for polar as well as non-polar systems. Both solutions must be examined separately. Important for the validity of both theories is the question, are the double layers in the system are overlapped or isolated? Thus the most important parameter is the  $\kappa a$ -value.

### Advanced CVI-theory for polar systems [10, 11]

It has been derived from the O'Brien theory mentioned above [8]. It postulates a correlation between the measured acoustic signal (CVI) and the dynamic electrophoretic mobility  $\mu_d$ .

$$CVI = A(\omega) \cdot F(Z_T, Z_S) \cdot \varphi \cdot \frac{\rho_p - \rho_m}{\rho_m} \cdot \mu_d \cdot \nabla P \quad \text{and (5)}$$

$$\mu_d = \frac{2\epsilon_m \epsilon_0 \zeta}{3\eta} \cdot G(s) \cdot (1 + F(Du, \omega')) \quad (6)$$

Thereby  $A(\omega)$  is a device constant,  $F(Z_T, Z_S)$  is a function of the acoustic impedance of the receiver and dispersion,  $\varphi$  is the solids content,  $\rho_p$  and  $\rho_m$  are the densities of particle and medium and  $\nabla P$  defines the pressure gradient of the ultrasound wave. Furthermore  $G(s)$  is the frequency dependence of the particles and  $F(Du, \omega')$  the influence of the Maxwell-Wagner-polarisation of the double layer.

If one takes into account, that the functions  $G$  and  $F$  for concentrated systems are dependant on the particle concentration and switches on to polydisperse systems, the relation for the colloidal vibration current and the dynamic mobility is given by:

$$CVI = \sum_{i=1}^N CVI_i \quad \text{and (7)}$$

$$\mu_d = \frac{2\epsilon_m \epsilon_0 \zeta}{3\eta} \cdot \frac{(\rho_s - \rho_m) \rho_s}{(\rho_p - \rho_m) \rho_m} \cdot \sum_{i=1}^N G(s_i, \varphi) \cdot (1 + F_i) \quad (8)$$

These relations are valid for almost every polydisperse dispersion with a polar solvent and almost any concentration (< 50 Vol.-%). The next step now is to achieve the validity of this theory for all surface conductivities.

### Surface conductivity

The surface conductivity appears tangential to the particle surface (figure 5). It influences the migration speed or mobility respectively in external applied fields and is taken into account neither in the SDEL-theory nor in the Smoluchowski-theory for movements in the electric field.

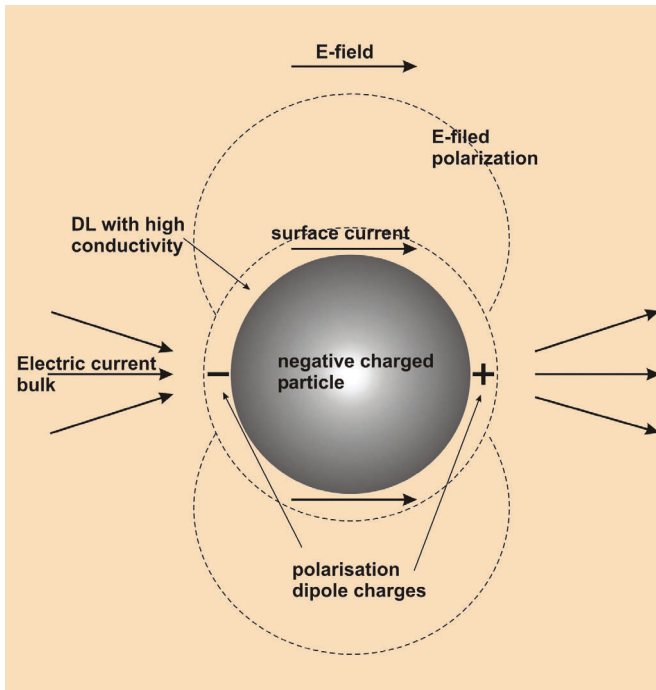


Figure 5 Surface conductivity of a particle

This effect is normally not limited to the shear plane. Thus it consists of two parts: the one of the bounded ions located in the stationary plane and the other of the diffuse layer [1]. The surface conductivity increases with an increasing ion concentration and an increasing zeta potential. The ion motion between the shear plane and the surface reduces the mobility of the particle. Thus too small zeta potentials are analysed using the SDEL-theory for such systems. The influence of the surface conductivity will be described by means of the Dukhin number  $Du$ , which can be written as:

$$Du = \frac{K^\sigma}{aK^L} \quad (9)$$

where  $K^\sigma$  is the surface conductivity,  $K^L$  is the conductivity of the electrolyte and  $a$  the particle radius. The surface conductivity increases significantly, the closer  $Du$  approaches the value of 1.

$$\mu_d = \frac{2\varepsilon_m \varepsilon_0 \zeta}{3\eta} \cdot \frac{(\rho_p - \rho_s) \rho_m}{(\rho_p - \rho_m) \rho_s} \cdot \sum_{i=1}^N G_i(s_i, \varphi_i) \cdot (1 + F_i(Du_i, \omega', \varphi)) \quad (10)$$

### Maxwell-Wagner relaxation – influence of the frequency

At a certain ultrasound frequency, the time period for the amplitude of the double layer is exactly identical to the diffusion time of the ions for the Debye length: Maxwell-Wagner frequency (MW-frequency). For this reason, fluctuations of the surface charge density must be taken into account for higher measurement-frequencies than this MW-frequency. This can't be done in case of the SDEL-theory. Thus it is just applicable for frequencies smaller than the MW-frequency. On the other hand, this effect will be considered in the „advanced CVI-theory for polar systems“ by means of a special function, which includes the so-called field induced surface charge density variation [10-11]. Mathematically this dependency is implemented in the function  $F_i(Du_i, \omega', \varphi)$ :

### Advanced CVI-theory for non-polar systems [13]

In case of non-polar systems the diffuse layer is expanding extremely although the permittivities are small. The reason for this is, that the number of charge carriers in the dispersion is low. The values of  $\kappa a$  are getting very small – depending on the solids content, an overlapping of the double layers is most likely. In strong non-polar systems, the double layers overlap already at a concentration of 0,04 %. The SDEL- as well as the advanced-theory described above is not valid for this case. Shilov et. al. developed a theory for such systems with overlapping double layers [13]. They determined the following correlation for the dynamic electrophoretic mobility:

$$\mu_d = \frac{2\varepsilon_m \varepsilon_0 RT}{9\eta \Omega F} \cdot (\kappa a)^2 \cdot \frac{1-\varphi}{\varphi} \cdot \sinh \frac{F\zeta}{RT} \cdot \frac{\rho_m}{\rho_s + i\omega(1-\varphi)} \cdot \frac{2a^2}{9\eta \Omega} \cdot \frac{\rho_p \rho_m}{\rho_p \rho_m} \quad (11)$$

where  $\Omega$  is a coefficient well known from the Stokes law ( $F = 6\pi\eta a \Omega v$ ). As can be concluded from equation (11), the mobility here is a function of the zeta potential  $\zeta$  and the volume fraction  $\varphi$ . Thus it is necessary to distinguish between cases of a thin double layer and thick double layer. In case of thin double layers, the surface charge density and the zeta potential are pure surface properties, independent of the volume fraction of the dispersed phase. In case of thick double layers the following relation between surface charge  $\sigma$  and zeta potential  $\zeta$  is valid:

$$\sigma = \frac{1}{3} \cdot \frac{RT}{F} \cdot \frac{1-\varphi}{\varphi} \cdot \varepsilon_m a \kappa^2 \sinh \tilde{\zeta} \quad (12)$$

Thus, in case of thick double layers, the zeta potential is not a pure surface property any more, but is additionally dependent on the solids content. This can lead to wrong conclusions regarding ion adsorption at colloidal surfaces. Because of that the specification of the zeta potential as well as the relevant surface charge (the real parameter of the surface properties) are necessary.



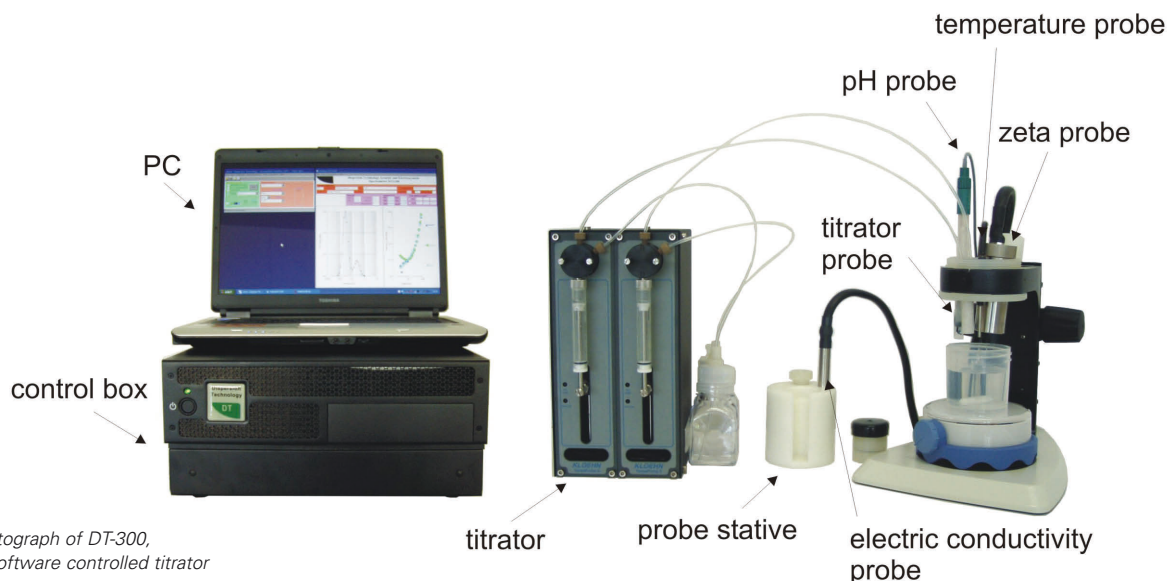


Figure 6 Photograph of DT-300, including the software controlled titrator

### Technical performance: The electroacoustic measurement probe DT-300

By means of the DT-300 in the configuration, as seen in figure 6, pH, electric conductivity and temperature can be measured parallel to the zeta potential. The software controlled titrator allows the determination of all measurement parameters in dependence on the pH, the additive-amount or the experiment time.

The measurement of the zeta potential works as shown in figure 3. The zeta potential probe (figure 7) consists of a stainless steel electrode, which also acts as a protection cover, a gold electrode and a ceramic isolation layer.

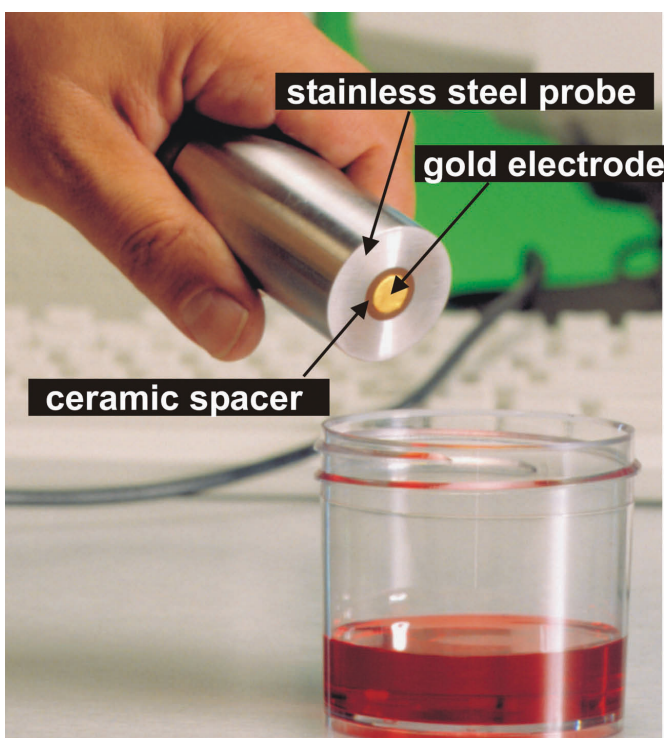


Figure 7 Zeta potential probe

The transmitted ultrasound wave has got a wave length of 3 MHz by default, because it is most commonly used in most applications. But it is also possible to vary the frequency. At least 800 sound pulses will be send into the sample. This number can be increased up to 1,6 million pulses in case of a very low signal or if the dispersion is not stable. In analogy to the particle size measurement via ultrasound attenuation, the zeta potential can be measured in flowing or a stationary dispersion.

### Execution and analysis of a measurement of the colloidal properties using the DT-300

To execute a measurement of the colloidal properties by means of the electroacoustic device DT-300, the material-phases of the dispersion must be defined and then be put into the database once. The required parameters of the liquid phase are density, dynamic viscosity and permittivity. For the dispersed phase just the density is required. Furthermore the fraction of the dispersed phase of the total system must be known. The electroacoustic measurement results of a nano-sized silica dispersion are given in figure 8.

The values with black letters in the field „CVI experiment and input“ are measurement values, those in blue are calculated parameters. „Magnitude“ is the amplitude of the colloidal vibration current (CVI) and „phase“ is its phase shift to the launched ultrasound wave. The fields „size“ and „st.dev“ represent the mean value and standard deviation of the dispersed phase. These values can be input alternatively or calculated by means of the CVI measurement. For fine particles (ca. < 400 nm) the particle size distribution doesn't

Sample Definition			
0.1225	wt fraction of silica X	in	water
measured on	2006-08-08 08:44:27		
Sample ID	zeta only	File Name	temperature: 24.4 pH: 9.22 porosity/fractal: 3
CVI experiment and input		Classic theory	Conductivity
magnitude	1808471	size	0.1
d. mobility	83232	st dev	0.3
phase	182.66	%[rel]	-15.57
	size phase	ka	12195
		S/m	0.08
		Debye length	0.004

Figure 8 Electroacoustic measurement result of a 12,25 wt.-% nanosized silica dispersion

influence the zeta potential measurement or can be neglected. Just for the calculation of the  $\kappa a$ -value, it is necessary to input the particle size. For coarser particles on the other hand, the increasing inertia influences the measurement signal (correction value „size phase“). The parameter „d. mobility“ is the dynamic mobility of the particles calculated by means of equation (4). The electric conductivity in S/m of the sample can be found in the field „conductivity“. Furthermore, the Debye-length is calculated using equation (1) and  $\kappa a$  is the product of the reciprocal Debye-length and particle radius.

The SDEL- and advanced-CVI-theory described above enable characterisation of colloidal properties of almost all aqueous and non-polar dispersions. By default, the analysis will be done using the SDEL-theory. This can be applied for most cases without any problems. The restrictions for this theory are as follow:

1. It's only applicable, in case if the double layer thickness is much smaller than the particle size ( $\kappa a \gg 1$ , benchmark is  $\kappa a > 10$ ).
2. The surface conductivity is neglected: strictly speaking it's only valid for very small Dukhin numbers ( $Du \ll 1$ ).
3. It is valid just for isolated double layers. This means that the solids content is limited at a certain conductivity and particle size.

A graphical representation of these limitations can be seen in figure 9.

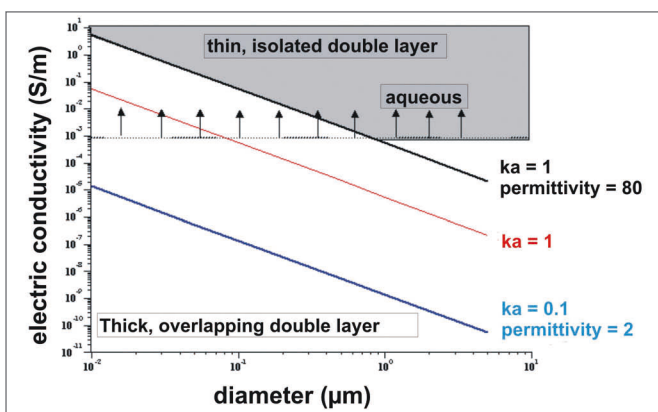


Figure 9 Scope of application of the SDEL-theory

If the SDEL-theory is not valid, the advanced-CVI-theories for polar and non-polar solvents must be applied. The double layer thickness and the Dukhin number can be determined if one knows the electric conductivity of the dispersion. For the advanced-CVI-theory for polar systems, the restrictions 2 and 3 of the SDEL-theory are invalid. This advanced theory is applicable for electric conductivities  $> 0,001$  S/m. For strong non-polar systems (electric conductivity  $< 0,001$  S/m) the theory according to Shilov is valid (see above). Thus the electric conductivity of the dispersion must be known in order to be able to apply the advanced-CVI-theories correctly.

For the presented measurement in figure 8, the results of the zeta potential of the SDEL- (Classic) and advanced-CVI-theory

Sample Definition		0.1225		refraction of silica X	in	water	measured on	2006-08-08 09:44:27
Sample ID	zeta only	File Name		temperature	24.4	pH	9.22	porosity/fractio
CVI experiment and input		- Classic theory		Conductivity	Advanced CVI approx.	Non-aqueous, Nano-colloids		
magnitude	1.003471	size	0.1	S/m	0.08	$\epsilon$	18.90	charge 10.927om
d. mobility	1.63232	std dev	0.3	(mV)	15.57	Die	0.1795	charge per particle
phase	162.66	size phase	0.14	Debye length	0.0041	charge	0.667	charges per particle
				$\kappa a$	12.152	$\zeta$ (mV)		

Figure 10 Analysis of the zeta potential of the example presented in figure 7

are given in figure 10. The  $\hat{\lambda}$ -value is close to 10. Thus the SDEL-theory is not applicable and the true value for the zeta potential is  $-19,98$  mV.

For the most applications the preconditions of the SDEL-theory are satisfied – then the differences with the advanced theory are marginal. The advanced-theories on the other hand are valid for almost all types of dispersion. For their application just the electric conductivity is necessary. Thus this parameter is often measured in parallel.

### Conclusion

A near-process measurement of the colloidal properties (in particular the zeta potential) of concentrated dispersions can be carried out by means of the electroacoustics. For a correct calculation, the knowledge of the fraction of the dispersed phase is necessary. Furthermore the density contrast between the continuous- and the dispersed phase and the permittivity of the medium must be known. The electroacoustic devices DT-300 and DT-1200 are measuring the colloidal vibration current using a special sender-detector probe via a pulse-echo-method. The software uses the most modern theories to describe the relationship between the measured parameters CVI and electric conductivity and the other set of parameters zeta potential, Debye-length, Dukhin number and dynamic mobility. This allows the characterization in the most polar and non-polar solvents.

### Literature

- [1] Lagaly, G.; Schulz, O.; Zimehl, R., „Dispersionen und Emulsionen“, Steinkopf, Darmstadt, ISBN 3-7985-1087-3 (1997).
- [2] Debye, P., „A method for the determination of the mass of electrolyte ions“, J. Chem. Phys., (1933), 13-16.
- [3] Hermans, J., Philos. Mag., 25, 426 (1938).
- [4] Rutgers, A. J.; Rigole W., „Ultrasound vibration potentials in colloid solutions, in solutions of electrolytes and pure liquids“, Trans. Faraday. Soc., 54, 139-143 (1958).
- [5] Booth, F. and Enderby, J. “On Electrical Effects due to Sound Waves in Colloidal Suspensions”, Proc. of Amer. Phys. Soc., 208A, 32 (1952).
- [6] Marlow, B.J., Fairhurst, D. and Pendse, H.P., “Colloid Vibration Potential and the Electrokinetic Characterization of Concentrated Colloids”, Langmuir, 4,3, 611-626 (1983).
- [7] Levine, S.; Neale, G.H., „The Prediction of Electrokinetic Phenomena within Multiparticle Systems. 1. Electrophoresis and Electroosmosis“, J. Coll. Interface Sci., 47, 520-532 (1974).
- [8] O'Brien, R.W. “Electro-acoustic Effects in a dilute Suspension of Spherical Particles”, J. Fluid Mech., 190, 71-86 (1988).
- [9] M. v. Smoluchowski, Elektrische Endosmose und Strömungsströme, in: Handbuch der Elektrizität und des Magnetismus, L. Graetz, Editor. (1921), Leipzig, S. 366-387.
- [10] Dukhin, A.S., Shilov, V.N., Ohshima, H., Goetz, P.J. “Electroacoustics Phenomena in Concentrated Dispersions. New Theory and CVI Experiment”, Langmuir, 15, 20, 6692-6706, (1999).
- [11] Dukhin, A.S., Shilov, V.N., Ohshima, H., Goetz, P.J. “Electroacoustics Phenomena in Concentrated Dispersions. Effect of the Surface Conductivity”, Langmuir, 16, 2615-2620 (2000).
- [12] Lyklema, J., „Fundamentals of Interface and Colloid Science“, vol. 1-3, Academic Press, London-NY, 1995-2000.
- [13] Shilov, V.N., Borkovskaja, Yu.B., and Dukhin A.S. “Electroacoustic theory for concentrated colloids with arbitrary  $\kappa a$ . Nano-colloids. Non-aqueous colloids.”, J. Coll. Interface Sci., submitted.

## News – Measuring the visco-elastic properties using the acoustic rheometers DT-600 and DT-1200

### Introduction

The determination of the visco-elastic properties of dispersions can be done by means of modern shear rheometers via oscillation measurements. The upper limit of the classical frequency range is about 1000 Hz. But how do such systems react when they are stressed with much higher frequencies? The answer for this question is one of the main topics of the acoustic rheometry. The application of acoustic waves allows an investigation of the visco-elastic properties of dispersions in the range of 1 to 100 MHz. In this sense, it is a complementary technique to the classical shear rheometers. A special advantage is the possibility to characterize systems which are susceptible to mechanical forces like gel structures non-destructively. Furthermore it is possible by means of this method to determine difficult to define parameter like the bulk viscosity. New information about rotation- and oscillation-degrees of freedom of molecules can be gained by knowing this value. You will find below the description of the new acoustic rheometer DT-600 followed by examples of possible applications. A short overview of the basics of oscillating rheological measurements can be found in the last chapter.

### Extensional viscosity measurements by means of the acoustic rheometer DT-600

#### Correlation between acoustic attenuation and rheology

Oscillation measurements can be carried out using modern shear viscosimeters. The cyclic stress will be induced by e.g. a rotating cylinder of plate, which frequency is in the hertz-range. The shear strain, which starts at the plate-dispersion boundary will be applied to the total system in one direction because of the low frequency, that is in the first half cycle of the oscillation.

Increasing the stress frequency significantly leads to a contrarwise stress of different areas. This is possible with acoustic waves, because they are compression waves, which are cyclic compressing some parts of the dispersion, while some other parts are expanded at the same time. To describe an acoustic compression wave mathematically, it's normally done by using the complex notation. The pressure  $p$  of the wave at a certain time  $t$  and a certain place is given by

$$P(x,t) = P_0 e^{-\alpha x} e^{i(\omega t - \omega x / v)} \quad (1)$$

where  $P_0$  is the initial pressure of the wave,  $\alpha$  the acoustic attenuation (in Np/m),  $v$  the sound speed (in m/s) and  $\omega$  the frequency of the oscillation (in Hz).  $\omega$  is in the range of Megahertz, which is a  $10^4$ -times faster stress than in case of a shear rheometer. It should be mentioned here, that the cyclic load of an ultrasound wave is not a pure shear stress.

It is different from a static compression load as well. In the literature this oscillating stress can be found as „longitudinal“ [2].

Furthermore it should be remarked, that a longitudinal modulus  $M^*$  was defined by Litovitz and Davis, similar to the  $G^*$  modulus [3]. The most important relations are the same for both. Thus the same denotation can be used when taking into account the type of stress in the index. Below are the symbol used for this modulus.

The elastic part  $G'_{long}$  and the loss part  $G''_{long}$  are resulting from the relations [4]:

$$G'_{long} = \rho \omega^2 v^2 \frac{\omega^2 - \alpha_{long}^2 v^2}{[\omega^2 + \alpha_{long}^2 v^2]^2} \quad \text{and} \quad (2)$$

$$G''_{long} = \rho \omega^2 v^2 \frac{\alpha_{long} v}{[\omega^2 + \alpha_{long}^2 v^2]^2} \quad (3)$$

There are two main differences in using longitudinal- or shear waves:

1. The depth of penetration is much bigger for longitudinal waves. For a frequency of 100 MHz in water, it is just 1  $\mu\text{m}$  for shear waves, while it is about 10 cm for longitudinal waves. The depths decreases with an increasing frequency for both types of waves. Thus longitudinal waves can be used in a much broader frequency range.
2. The essential difference is the nature of load [5]: for shear loads, just the classical dynamic viscosity  $\eta$  is important, because it only initialises the translatory motion of the molecules. In case of a longitudinal load, additional rotation- and oscillating motions are activated. Hence the detection of rotation- and oscillation effects in complex liquids can be realized only by means of longitudinal waves.

For Newtonian liquids, the viscosity is independent of the load (shearing, compression) constant. In case of the acoustic rheology this means, that the attenuation shows a linear dependency of the frequency. The relation between the longitudinal wave and the viscosity of a Newtonian liquid is given by the Navier-Stokes-equation [6]

$$\rho \left[ \frac{\partial v}{\partial t} + (v \nabla) v \right] = -\text{grad}P + \eta \Delta v + \left( \eta^b + \frac{4}{3} \eta \right) \text{grad} \text{div} v \quad (4)$$

where  $\rho$  is the density,  $t$  the time,  $v$  the speed of the fluid,  $P$  the pressure of the wave and  $\eta$  the dynamic viscosity. In this rather complex equation, the right hand side term takes into account liquid compressibility. The additional parameter  $\eta^b$  is the volume- or bulk viscosity. For most rheological tests,

the liquid will be assumed as incompressible and the volume viscosity doesn't play a role. For an incompressible liquid the Navier-Stokes-equation will be reduced to

$$\rho \left[ \frac{\partial \mathbf{v}}{\partial t} + (\mathbf{v} \cdot \nabla) \mathbf{v} \right] = -\text{grad}P + \eta \Delta \mathbf{v} \quad (5)$$

According to Stokes the following relation between attenuation  $\alpha_{\text{long}}$  and viscosity  $\eta$  results from equation (12) for Newtonian, incompressible liquids [7]

$$\alpha_{\text{long}} = \frac{2\omega^2 \eta}{3\rho v^3} \quad (6)$$

and for compressible liquids [2]

$$\alpha_{\text{long}} = \frac{2\omega^2}{3\rho v^3} \left[ \frac{4}{3}\eta + \eta^b \right] \quad (7)$$

On the basis of these relations, a longitudinal viscosity can be defined, which describes the energy losses in a longitudinal wave. The following equations are valid:

$$\eta_{\text{long}} = \frac{4}{3}\eta + \eta^b \quad \text{for Newtonian liquids} \quad (8)$$

and

$$\eta_{\text{long}} = \frac{2\alpha_{\text{long}} \rho v^3}{\omega^2} \quad \text{for non-Newtonian liquids} \quad (9)$$

Obviously the longitudinal viscosity is frequency dependent for non-Newtonian liquids but independent for Newtonian liquids.

To summarize, the following measurement can be obtained by means of acoustic rheology:

1. Newtonian liquids can be characterized regarding their dynamic viscosity using equation (6).
2. Newtonian tests can be carried out by means of a measurement of the acoustic attenuation spectrum ( $\alpha_{\text{long}}$  vs.  $\omega$ ).
3. If the dynamic viscosity  $\eta$  of a certain liquid is known, the volume viscosity  $\eta^b$  can be determined via equation (7).
4. The elastic- and loss modulus  $G'_{\text{long}}$  and  $G''_{\text{long}}$  of a dispersion can be determined using equation (2) and (3).

### Technical performance: The acoustic rheometer DT-600 and DT-1200

The dispersion (or alternatively a pure liquid) will be purred into the measurement chamber of the DT-600 and its acoustic attenuation will be measured (figure 1). Also the sound speed will be measured. By means of the titrator, these measurements can be taken at different pH values or with different amounts of additive.

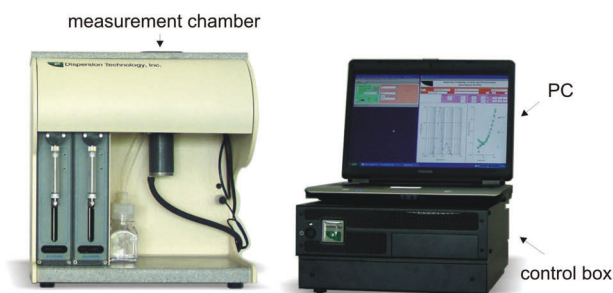


Figure 1 Acoustic rheometer DT-600

The measurement of the acoustic attenuation occurs in analogy to the particle size determination in a frequency range of 1 to 100 MHz and at different sender-detector gaps (18 frequencies, 21 gaps) The acoustic attenuation coefficient is defined as:

$$\alpha_{\text{exp}} [\text{dB/cm/MHz}] = \frac{10}{f[\text{MHz}]L[\text{cm}]} \log \frac{I_{\text{in}}}{I_{\text{out}}} \quad (10)$$

were  $f$  is the frequency of the pulse and  $L$  the gap between sender and detector. The sound speed will be determined using the time-of-flight principle: the instrument is measuring the time delay of the emitted and detected wave for different gaps. The sound speed results from the linear dependency  $c = L/t$ . It will be required for a chronological optimal sequence of the ultrasound pulses. Additionally the instrument is equipped with probes to measure and to control the temperature.

### Execution of a rheological test using the DT-600

#### Newtonian-Test

After filling the measurement chamber with the dispersion, the attenuation spectrum will be measured between 1 and 100 MHz. In figure 2 the spectra of deionised water are shown in comparison with a 10 wt-% polymer dispersion.

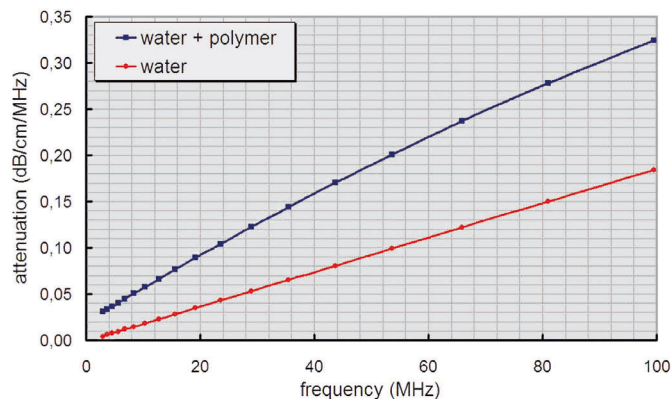


Figure 2 Measured acoustic attenuation spectrum (water and polymer dispersion) for rheological test

On the basis of these spectra  $\alpha_{\text{exp}}$  (dB/cm / MHz) vs.  $f$  (MHz) can be concluded, if a liquid behaves Newtonian or non-Newtonian. In case of a Newtonian liquid (water), the attenuation shows a linear dependency of the frequency. The wave frequency  $\omega$  depends on the angular frequency  $\lambda$  and the wave length via

$$\lambda = \frac{2\pi V}{\omega} = \frac{V}{f} \quad (11)$$

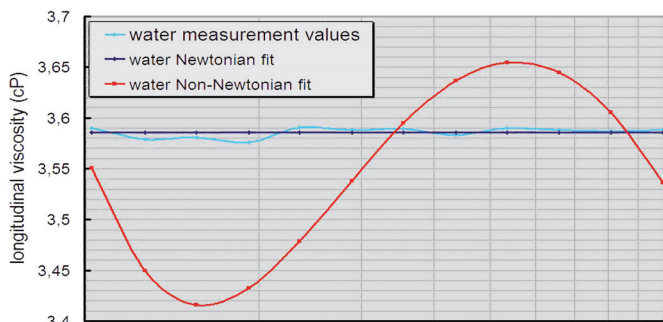


Figure 3 Specific Newtonian-test for the Newtonian liquid water

Alternatively a specific Newtonian-test can be carried out: for this purpose the frequency specific attenuation values are converted into the longitudinal viscosity  $\eta_{\text{long}}$  using equation (9). For Newtonian liquids,  $\eta_{\text{long}}$  is a constant, independent of the frequency,  $t$ . In figure 3, the Newtonian test for water (a Newtonian liquid) is shown.

By default the test will be executed in the frequency area 10 – 100 MHz, because at lower frequencies the wave length is comparable to the sender-detector gap distance (e.g. 1,5 mm at 1 MHz). Thus diffraction effects arise, which requires a special geometrical calibration of the cell for the lower frequencies (1 to 10 MHz). The frequency range 10 – 100 MHz is independent from the calibration and thus will be used for the Newtonian test. Furthermore the following rule is valid: the stronger the total attenuation of the liquid (e.g. for higher concentrated systems), the lower the influence of the wave diffraction and it can be neglected. This is similar to the particle size measurement.

### Measurement of the bulk viscosity

During the test, a special statistic procedure is used to distinguish, if a liquid or dispersion is Newtonian or non-Newtonian. A more detailed paper on this topic can be found in [2]. In doing this, the dynamic viscosity  $\eta^p$  of the solid/dispersion must be known. The equation (12, in SI-terms) results from equation (7):

$$\eta^b \left[ \frac{\text{kg}}{\text{m} \cdot \text{sec}} \right] = \frac{2\alpha_{100\text{MHz}} [\text{dB/cm/MHz}] \cdot \rho [\text{kg/m}^3] \cdot v^3 [\text{m/sec}]}{4\pi \cdot 8.69 \cdot 10^{12}} - \frac{4}{3} \eta \left[ \frac{\text{kg}}{\text{m} \cdot \text{sec}} \right] \quad (12)$$

It can be estimated, that the bulk viscosity is a much more sensitive parameter for the molecular structure of the liquid than the dynamic viscosity [2]. Some examples are given in table (1). There seems to be no correlation between these two parameters also.

### Determination of storage-, loss modulus and compressibility

Storage modulus  $G'$ , loss modulus  $G''$  (in dependence on frequency) and compressibility of the liquid/ dispersion can be calculated easily by means of the equations (2), (3) and the measured sound speed (table 1).

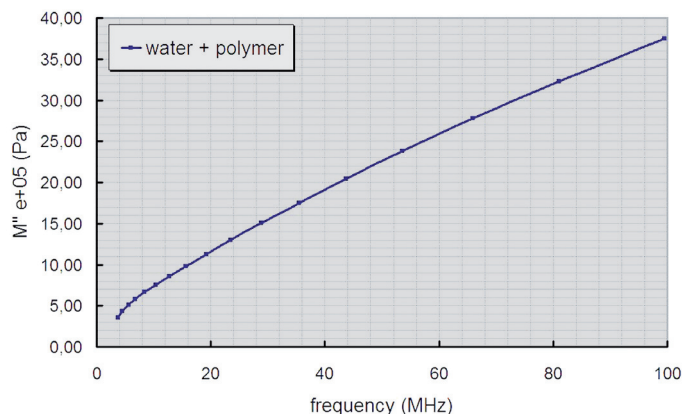


Figure 4 Calculation of the loss modulus  $G''$  on the basis of the attenuation spectrum of the polymer dispersion of figure 2

Liquid	Attenuation 100 MHz, 25°C (dB/cm/MHz)	Dynamic viscosity (published value in cP)	Bulk viscosity (cP)	Sound speed (m/sec)	compressibility E10 (1/Pa)	Storage modulus $G'$ E09 (Pa)
water	0.186	0.89	2.43	1496	0.63	2.23
ethanol	0.42	1.074	1.47	1147	1.36	1.03
hexane	0.6	0.3	2.49	1078	1.84	0.77
toluene	0.72	0.56	7.69	1308	0.92	1.53
cyclohexane	2.07	0.894	17.43	1256	1.15	1.23

Table 1 Attenuation coefficient, storage modulus, compressibility, sound speed, dynamic- and bulk viscosity of different Newtonian liquids at 25 °C [2]

**Some basics of oscillating rheological measurements (appendix)**

Dispersions have got elastic characteristics besides their viscous properties. Most of the pure liquids show a mainly viscous character with only limited elastic parts. The elasticity of a liquid contains information about structures inside the material: a low elasticity means weak structures.

The sum of all these mechanical properties, the so called „visco-elastic properties“ can be mathematically described as shown in figure 5: elastic parts are represented by spring elements, viscous parts by damping elements.

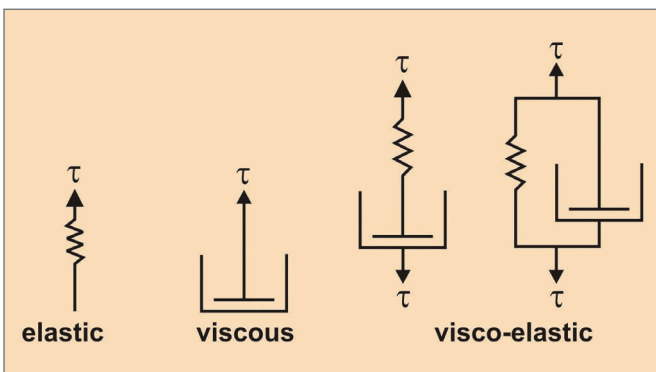


Figure 5 Description of visco-elastic properties by spring- and damping elements

Visco-elastic properties can be investigated not by means of static deformation experiments but by other load types. A very beneficial method is oscillation loads, its characteristic will be discussed below.

In case of an oscillating load, a small periodic, mostly sinusoidal shear stress  $\tau$  is applied to a dispersion – the reaction will be an also periodic deformation  $\gamma$  of the dispersion. The amplitude of the elongation is small to keep the measurement in the linear visco-elastic range (see below).

The assumption for the following calculation is, that a small periodic shear stress  $\tau$  with a frequency  $f$  is applied to a dispersion. The answer of the dispersion to this load is an also periodic strain  $\gamma$  with the same frequency  $f$ , but normally not in-phase. This means that there will be a characteristic phase shift  $\theta$  between  $\tau$  and  $\gamma$ . If one take into account that the relation between the oscillation frequency  $f$  and the angular frequency  $\omega$  is  $\omega = 2\pi f$ , it can be written as:

$$\gamma(t) = \gamma_0 \cos \omega t \quad \text{and} \quad \tau(t) = \tau_0 \cos(\omega t - \theta) \quad (13)$$

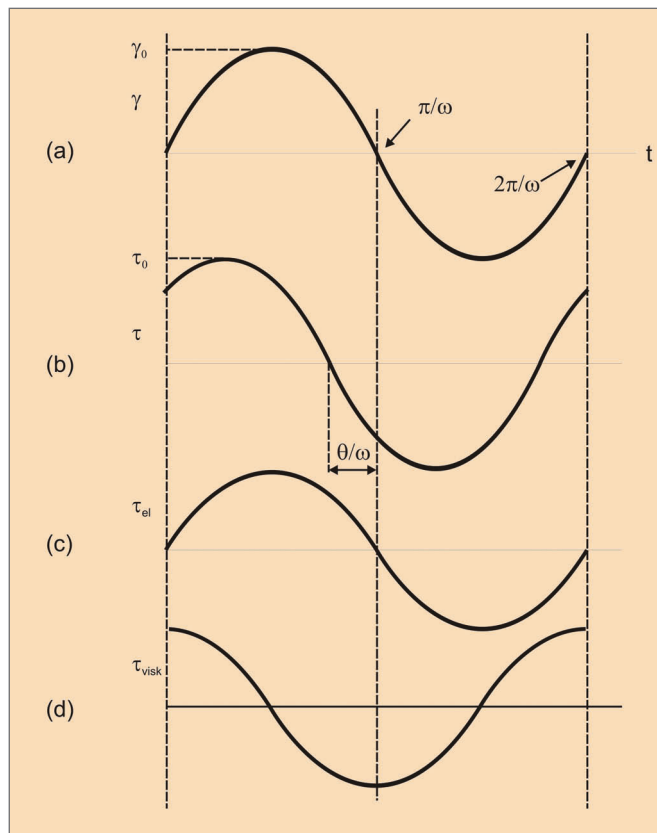


Figure 6 Oscillating experiment – stress and strain

In figure 6 (a) and (b) this situation is shown graphically [1].

Normally it is convenient to write these angular functions as complex variables (projection on the area level). Stress and strain can be written as

$$\gamma^* = \gamma_0 e^{i\omega t} \quad \text{and} \quad \tau^* = \tau_0 e^{i(\omega t - \theta)} \quad (14)$$

where  $\tau_0$  and  $\gamma_0$  are the maximum stress and strain respectively. These relations are valid only in the visco-elastic range, Outside this range, the relation between these two parameters is given by

$$\tau^* = G^* \gamma^* \quad (15)$$

where  $G^*$  is the so called complex shear modulus. Substitution ((14) in (15)) and taking into account the relation  $e^{-i\theta} = \cos\theta - i \cdot \sin\theta$ ,  $G^*$  can be written as

$$G^* = \frac{\tau_0}{\gamma_0} e^{-i\theta} = \frac{\tau_0}{\gamma_0} (\cos \theta - i \sin \theta) = G' - iG'' \quad (16)$$

with

$$G' = \frac{\tau_0}{\gamma_0} \cos \theta \quad \text{and} \quad G'' = \frac{\tau_0}{\gamma_0} \sin \theta$$

$G'$  is the so called storage modulus or elastic part,  $G''$  the shear modulus or viscous part. The relation

$$\tan \theta = \frac{G''}{G'} \quad (17)$$

specifies the amount of elastic and viscous properties of a material.

This mathematical construct must be transferred now to the concept of the viscosity. First the viscosity  $\eta$  is defined as the proportionality factor between shear stress  $\tau$  and shear rate  $\dot{\gamma}$ :

$$\tau = \eta \dot{\gamma} \quad \text{with} \quad \dot{\gamma} = \frac{d\gamma}{dt} \quad (18)$$

If one determines the shear rate of a periodic strain  $\gamma$ , one obtains

$$\dot{\gamma} = -\gamma_0 \omega \sin \omega t \quad (19)$$

According to this a complex viscosity  $\eta^*$  can be defined as

$$\eta^* = \eta' + i\eta'' \quad \text{with} \quad \eta' = \frac{G'}{\omega} \quad \text{and} \quad \eta'' = \frac{G''}{\omega} \quad (20)$$

It should be noted, that the phase shift  $\theta$  between applied stress and measured strain will be zero for a pure elastic material. In case of an ideal viscous (Newtonian) liquid, one obtains:  $\eta' = \eta$  and  $\eta'' = 0$ . Then the phase shift  $\theta$  between applied stress and measured strain is exactly  $90^\circ$ .

#### Literature

- [1] Van Vliet, T.; Lyklema, J., „Rheology“, In „Fundamentals of Interface and Colloid Science – VOLUME IV: PARTICULATE COLLOIDS“, Elsevier, 2005, 6.1 – 6.89, ISBN: 0-12-460529-X.
- [2] Dukhin, A. S.; Goetz, P. J., „Rheology and Acoustics“, to be published.
- [3] Litovitz, T. A.; Davis, C. M., In „Physical acoustics“, Ed. W. P. Mason, vol. 2, chapter 5, Academic Press, New York.
- [4] Williams, P. R.; Williams, R. L., „The determination of dynamic moduli at high frequencies“, J. of Non-Newtonian Fluid Mechanics, 42, 267-282, 1992.
- [5] Temkin, S., „Elements of Acoustics“, Acoustical Society of America, 2001.
- [6] Morse, P. M.; Ingard, K. U., „Theoretical Acoustics“, Princeton University Press, MJ, 1986.
- [7] Stokes, K. K., „On the theories of the internal friction in fluids in motion, and of the equilibrium and motion of elastic solids“, Transactions of the Cambridge Philosophical Society, vol. 8, 22, pp. 287-342, 1845.

#### Imprint

Editor:  
 QUANTACHROME GmbH & Co. KG  
 Rudolf-Diesel-Straße 12  
 D-85235 Odelzhausen  
 Phone +49 8134-9324-0  
 Fax +49 8134-9324-25  
 info@quantachrome.de  
 www.quantachrome.eu.com

Editorial Staff:  
 Dr. Christian Oetzel, Dr. Dietmar Klank

Illustrations:  
 Quantachrome GmbH & Co. KG, Fotolia

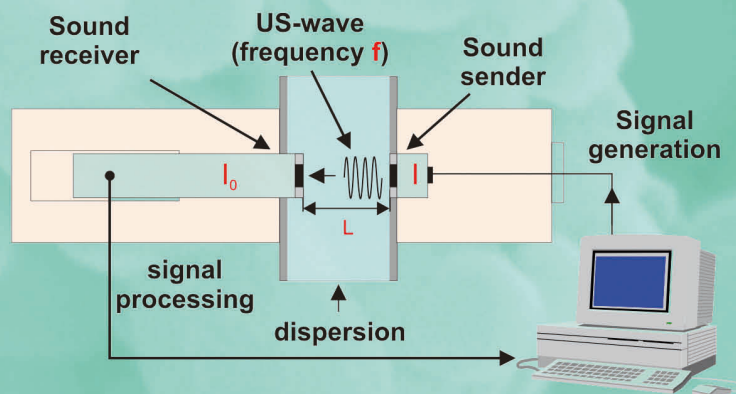


## Characterization of Dispersions and Powders



# Ultrasound for characterization of dispersions

## Ultrasound spectrometry



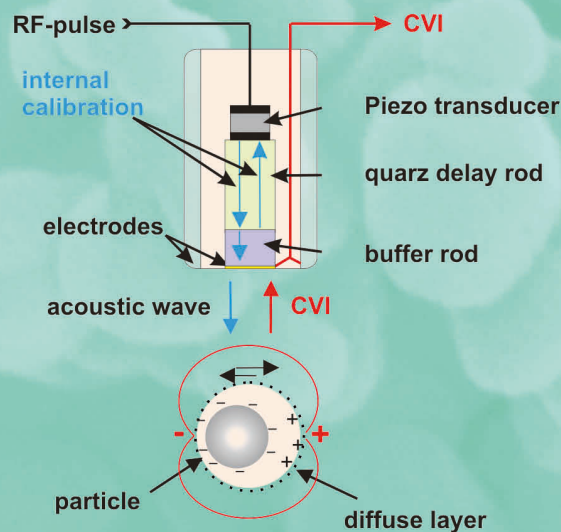
**DT-1200 and DT-100:**

Particle size in concentrated dispersions

**DT-1200 and DT-600:**

visco-elastic properties of  
dispersions in megahertz range - nondestructive

## Electroacoustic



**DT-1200 and DT-300:**

Zeta potential in concentrated dispersions

**Quantachrome**  
Your partner in  
particle characterization

[www.quantachrome.eu.com](http://www.quantachrome.eu.com)